Naturalis Repository

Multilocus species tree analyses resolve the radiation of the widespread Bufo bufo species group (Anura, Bufonidae)

E. Recuero, D. Canestrelli , J. Vörös, K. Szabó , N.A. Poyarkov, J.W. Arntzen,
J. Crnobrnja-Isailovic, A.A. Kidov, D. Cogălniceanu, F.P. Caputo, G. Nascetti,
I. Martínez-Solano

Downloaded from
https://doi.org/10.1016/j.ympev.2011.09.008

Article 25fa Dutch Copyright Act (DCA) - End User Rights

This publication is distributed under the terms of Article 25fa of the Dutch Copyright Act (Auteurswet) with consent from the author. Dutch law entitles the maker of a short scientific work funded either wholly or partially by Dutch public funds to make that work publicly available following a reasonable period after the work was first published, provided that reference is made to the source of the first publication of the work.

This publication is distributed under the Naturalis Biodiversity Center 'Taverne implementation' programme. In this programme, research output of Naturalis researchers and collection managers that complies with the legal requirements of Article 25fa of the Dutch Copyright Act is distributed online and free of barriers in the Naturalis institutional repository. Research output is distributed six months after its first online publication in the original published version and with proper attribution to the source of the original publication.

You are permitted to download and use the publication for personal purposes. All rights remain with the author(s) and copyrights owner(s) of this work. Any use of the publication other than authorized under this license or copyright law is prohibited.

If you believe that digital publication of certain material infringes any of your rights or (privacy) interests, please let the department of Collection Information know, stating your reasons. In case of a legitimate complaint, Collection Information will make the material inaccessible. Please contact us through email: collectie.informatie@naturalis.nl. We will contact you as soon as possible.

Molecular Phylogenetics and Evolution 62 (2012) 71–86

Contents lists available at SciVerse ScienceDirect

Molecular Phylogenetics and Evolution

journal homepage: www.elsevier.com/locate/ympev

Multilocus species tree analyses resolve the radiation of the widespread *Bufo bufo* species group (Anura, Bufonidae)

E. Recuero[a], D. Canestrelli[b], J. Vörös[c], K. Szabó[c], N.A. Poyarkov[d], J.W. Arntzen[e], J. Crnobrnja-Isailovic[f,g], A.A. Kidov[h], D. Cogălniceanu[i], F.P. Caputo[b], G. Nascetti[b], I. Martínez-Solano[j,*]

[a] Museo Nacional de Ciencias Naturales, CSIC, c/ José Gutiérrez Abascal, 2, 28006 Madrid, Spain
[b] Department Ecology and Biology, Tuscia University, Largo dell'Università s.n.c., I-01100 Viterbo, Italy
[c] Hungarian Natural History Museum, 1088 Budapest, Baross u. 13, Hungary
[d] Department of Vertebrate Zoology, Biological Faculty, Lomonosov Moscow State University, Leninskiye Gory, GSP-1, Moscow 119991, Russia
[e] Netherlands Centre for Biodiversity Naturalis, P.O. Box 9517, 2300 RA Leiden, The Netherlands
[f] Department of Biology and Ecology, Faculty of Sciences and Mathematics, University of Niš, Višegradska 33, 18000 Niš, Serbia
[g] Institute for Biological Research "Siniša Stanković", University of Belgrade, Despota Stefana 142, 11000 Belgrade, Serbia
[h] Russian State Agrarian University – Moscow Timiryazev Agricultural Academy, Timiryazevskaya Str., 49, 127550 Moscow, Russia
[i] University Ovidius Constanta, Faculty of Natural Sciences, Bvd. Mamaia 124, Constanta, Romania
[j] Instituto de Investigación en Recursos Cinegéticos (CSIC-UCLM-JCCM), Ronda de Toledo, s/n, 13005 Ciudad Real, Spain

ARTICLE INFO

Article history:
Received 5 July 2011
Revised 7 September 2011
Accepted 11 September 2011
Available online 22 September 2011

Keywords:
Amphibia
Bufo bufo
Bufo spinosus
Mitochondrial DNA
Nuclear DNA
Species trees

ABSTRACT

New analytical methods are improving our ability to reconstruct robust species trees from multilocus datasets, despite difficulties in phylogenetic reconstruction associated with recent, rapid divergence, incomplete lineage sorting and/or introgression. In this study, we applied these methods to resolve the radiation of toads in the *Bufo bufo* (Anura, Bufonidae) species group, ranging from the Iberian Peninsula and North Africa to Siberia, based on sequences from two mitochondrial and four nuclear DNA regions (3490 base pairs). We obtained a fully-resolved topology, with the recently described *Bufo eichwaldi* from the Talysh Mountains in south Azerbaijan and Iran as the sister taxon to a clade including: (1) north African, Iberian, and most French populations, referred herein to *Bufo spinosus* based on the implied inclusion of populations from its type locality and (2) a second clade, sister to *B. spinosus*, including two sister subclades: one with all samples of *Bufo verrucosissimus* from the Caucasus and another one with samples of *B. bufo* from northern France to Russia, including the Apennine and Balkan peninsulas and most of Anatolia. Coalescent-based estimations of time to most recent common ancestors for each species and selected subclades allowed historical reconstruction of the diversification of the species group in the context of Mediterranean paleogeography and indicated a long evolutionary history in this region. Finally, we used our data to delimit the ranges of the four species, particularly the more widespread and historically confused *B. spinosus* and *B. bufo*, and identify potential contact zones, some of which show striking parallels with other co-distributed species.

1. Introduction

The long-term goal of Systematics is understanding the historical relationships among organisms, and a powerful tool to achieve this goal is to estimate robust species trees (Edwards, 2009). The importance of combining information from multiple, unlinked loci in individuals from a geographically comprehensive sample to obtain robust estimates of phylogenetic relationships has been long recognized. Recently, the increased availability of molecular data and the parallel development of efficient analytical tools to extract the information have increased the accuracy of species tree estimation (Liu et al., 2008; Kubatko et al., 2009; Heled and Drummond, 2010). New analytical tools are improving our ability to reconstruct species trees from multilocus datasets, despite difficulties associated with the processes of recent, rapid divergence, incomplete lineage sorting and/or introgression in phylogenetic reconstruction (Chung and Ané, 2011). For instance, methodological advances related to estimation of the timing of population divergence, and in particular the incorporation in the analyses of the uncertainty associated to estimates of substitution rates and the temporal constraints imposed by the fossil record have greatly improved our understanding about the timescales involved in species formation in a wide variety of taxonomic groups (for example, Aldenhoven et al., 2010; Arora et al., 2010; Blackburn et al., 2010). This has also led to taxonomic revision of historically

---

* Corresponding author. Fax: +34 926 295 451.
E-mail address: inigomsolano@irec.csic.es (I. Martínez-Solano).

1055-7903/$ - see front matter
doi:10.1016/j.ympev.2011.09.008

problematic groups, which include widespread and morphologically undifferentiated species (for example, Gvozdík et al., 2010; Salicini et al., in press; Sanguila et al., 2011).

Until recently, the genus *Bufo* contained some of the largest number of amphibian species in the world, with a total of 283 described toad species. As a result of its paraphyly it was split by Frost et al. (2006) into several genera. Far from adequately solving the systematics, this highlighted the complexity of the group. As an example, the green toad (*Bufo viridis*) that is widespread throughout Eurasia and parts of northern Africa, has a complex genetic structure, including differences in ploidy levels across species and populations (Stöck et al., 2006). It was split into several species, with additional changes in green toad taxonomy expected in the near future (Stöck et al., 2006, 2008). *Bufo bufo* (Linnaeus 1758) (Anura, Bufonidae), another widespread species with an extensive Euro-Asiatic distribution, was formerly included in the *B. bufo* species group of Inger (1972), including species from Europe through Asia. Recent studies have recognized a marked distinction between western and eastern species groups, some within the latter now recognized as distinct species, like *B. japonicus* (Matsui, 1980, 1984; Igawa et al., 2006) and *B. gargarizans* (Gumilevskij, 1936; Matsui, 1986; Macey et al., 1998; Liu et al., 2000; Fu et al., 2005). Here we focus on the western species group, including *B. bufo* and related species, that ranges from the Iberian Peninsula and North Africa in the west to northern Kazakhstan and eastern Siberia in the east (IUCN, 2009, Fig. 1). The boundaries of the different species and their phylogenetic relationships remain poorly known, and a recent study has shown that the actual species diversity in the group is underestimated (Litvinchuk et al., 2008), highlighting the need for more work.

Litvinchuk et al. (2008) described a new species from the Talysh Mountains in south Azerbaijan and Iran, *B. eichwaldi*, which is morphologically and genetically distinct from *B. bufo*, and discussed its relationships with *B. bufo* and *B. verrucosissimus*. However, their study lacked comprehensive sampling and did not include populations from western Europe, which in turn prevented a thorough re-evaluation of the status of *B. bufo* – in particular, the delineation of the ranges of the most widespread subspecies: *B. b. bufo* and *B. b. spinosus,* whose type localities are in Sweden and southern France, respectively (Frost, 2011). The three subspecies traditionally recognized in *B. bufo* (*B. b. bufo, B. b. gredosicola*, and *B. b. spinosus*) (Dubois and Bour, 2010) were originally described based on morphological differences. Additionally, Litvinchuk et al. (2008), based on allozyme data, suggested that the available name *B. b. palmarum* be used for the Italian populations of this species. In any case, the relative ranges and potential areas of overlap between the different subspecies remain unknown and their taxonomic status is disputed because of the lack of consistence of purported diagnostic characters across populations (see for instance De Lange, 1973; Lüscher et al., 2001; García-París et al., 2004). Preliminary mtDNA studies based on partial sequences of the control region did not find evidence for geographical structuring of populations of *B. bufo* in the Iberian Peninsula, where up to three subspecies have been reported; instead, the Iberian populations form a well-supported clade with respect to north African samples (Martínez-Solano and González, 2008). Within the Caucasian species *Bufo verrucosissimus*, three to four morphological subspecies are currently recognized (*B. v. verrucosissimus*, *B. v. turowi*, *B. b. circassicus*, and *B. b. tertyschnikovi*; see Orlova, Tuniyev, 1989; Kidov, 2009); but their taxonomic status remains questionable (Kuzmin, 1999; Litvinchuk et al., 2008). Also, the distribution limits of *B. verrucosissimus* and *B. bufo* in North Anatolia are unclear (Eiselt, 1965; Baran and Atatur, 1998).

In this paper, we present a comprehensive assessment of the diversification history of the *B. bufo* species group in Europe using molecular data from the mitochondrial and nuclear genomes, including all described species and subspecies with full geographic coverage. In particular, the objectives of our study are: (1) resolving phylogenetic relationships between species in the widespread *B. bufo* species group; (2) reconstructing well-dated

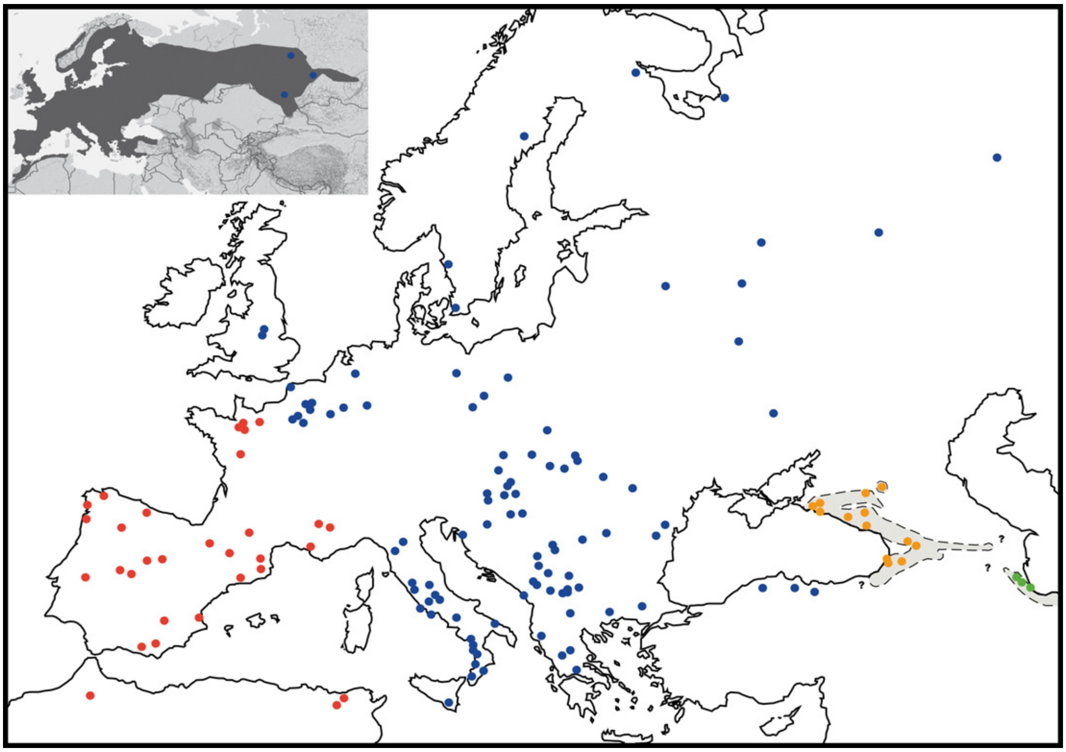

Fig. 1. Sampling localities (see also Table 1). Blue dots represent samples of *Bufo bufo*, and red dots, *B. spinosus*. The distribution of *B. bufo* and *B. spinosus* is shown in the inset, which shows also the location of the three easternmost samples in our dataset. The distributions of *B. verrucosissimus* (orange dots) and *B. eichwaldi* (green dots) are shaded. (For interpretation of the references to color in this figure legend, the reader is referred to the web version of this article.)

and robust paleobiogeographic scenarios for the evolution of the group, and (3) use this information to delineate the ranges of the species and identify potential contact zones.

2. Material and methods

2.1. Sampling and sequencing

A total of 232 individuals of *B. bufo sensu lato* (i. e., including all currently recognized subspecies) and related species (*B. verrucosissimus* and *B. eichwaldi,* including all currently recognized subspecies, see Kutrup et al., 2006; Litvinchuk et al., 2008; Sinsch et al., 2009) were included in the study (Table 1, Fig. 1). We collected samples across all the species ranges, with a focus in the three main southern peninsulas in Europe, and including populations from North Africa (Morocco and Tunisia), Caucasian isthmus and Anatolia. As outgroups we included nine samples from other species previously considered part of the *B. bufo* species group (in the "eastern species group" cited above): *B. bankorensis*, *B. gargarizans*, *B. japonicus*, and *B. torrenticola* (Table 1).

Genomic DNA was extracted from tissues (tail or toe clips), preserved in 95% ethanol or frozen, using commercial kits (Nucleospin). We amplified by polymerase chain reaction (PCR) and sequenced fragments of two mitochondrial genes (16S and cytochrome *b*, cyt-b) in all 241 samples, and four nuclear genes (proopiomelanocortin: POMC, chemokine (C-X-C) receptor 4: CXCR4, brain-derived neurotrophic factor: BDNF, and ribosomal protein L3: RPL3) in 52–55 samples representing all major mtDNA clades (see Table 1). PCR conditions followed standard procedures (see Martínez-Solano and González, 2008), with primers and annealing temperatures listed in Table 2.

2.2. Molecular diversity, neutrality and recombination tests

Number of haplotypes and values of mean haplotype (h) and nucleotide diversities (π) (Nei, 1987) for mtDNA (16S + cyt-b) were estimated within and between species using DnaSP v5.0 (Librado and Rozas, 2009). Genetic distances within and between species were calculated with MEGA5 (Tamura et al., 2011). To test whether the data were consistent with neutral expectations, we also calculated Tajima's D statistic (Tajima, 1989) and Fu and Li's (1993) D and F statistics for each locus using DnaSP. Recombination in the nuclear markers was assessed using the pairwise homoplasy index (PHI – Φ – statistic, Bruen et al., 2006) implemented in Splitstree v.4.11 (Huson and Bryant, 2006).

2.3. Phylogenetic analyses

For each data set (16S, cyt-b, POMC, CXCR4, BDNF and RPL3), the best-fit model of evolution was estimated based on the Bayesian Information Criterion (BIC) as implemented in jModeltest 1.0 (Guindon and Gascuel, 2003; Posada, 2008). Phylogenetic analyses were based on Bayesian inference, maximum likelihood (ML) and maximum parsimony (MP) methods as implemented in MrBayes v3.1.2 (Huelsenbeck and Ronquist, 2001), Garli version 2.0 (Zwickl, 2006) and PAUP∗ v4.10 (Swofford, 2001) respectively. Several independent analyses were run: (1) a combined mtDNA (16S + cyt-b) dataset including only one representative of each haplotype in the dataset; (2) a combined nDNA (POMC, CXCR4, BDNF and RPL3) dataset; and (3) a combined mtDNA + nDNA dataset. Bayesian and ML analyses were run with the different genes set as independent partitions, with the models selected by jModeltest. Support for branches was based on Bayesian posterior probabilities (BPPs) and bootstrap values for ML and MP analyses. For analyses with Garli, 100 bootstrap replicates were run, with five search replicates per bootstrap replicate. In PAUP, bootstrap values were estimated from 1000 replicates, with a maximum of 1000 (mtDNA, dataset 1) or 20,000 (datasets 2 and 3) trees saved per random addition replicate in order to keep computation time within reasonable bounds. Sequence alignments were deposited in TreeBase (http://purl.org/phylo/treebase/phylows/study/TB2:S11885).

We also estimated time to most recent common ancestor (TMRCA) of selected haplogroups in the mtDNA dataset, corresponding to each species as well as geographically based haplogroups where relevant using BEAST v1.6.1 (Drummond and Rambaut, 2007). For these analyses, we considered two partitions, one for each gene (16S and cyt-b), with substitution models selected based on jModeltest results, and a relaxed (uncorrelated-lognormal) clock model, since preliminary runs showed it fit the data better than a strict clock model (i.e., the 95% highest posterior density (HPD) interval for the parameter "coefficient of variation" did not include zero). We specified a substitution rate sampled from a normal distribution with a mean of 0.0069 and a standard deviation of 0.0017 substitutions per site per million years, based on rates estimated by Macey et al. (1998) in related species. We used fossil data as prior information to set bounds on some TMRCAs, based on the oldest fossil remains of *B. bufo* (*sensu lato*) and *B. verrucosissimus* in Europe (see Martín and Sanchiz, 2011). There are Miocene records from fossil sites in Moldavia (9.7–11.1 million years ago – Mya) that have been assigned to *B. bufo*. Since at present there are no diagnostic osteological features distinguishing between species in the *B. bufo* group (except for *B. verrucosissimus*, Chkhikvadze, 1984; Ratnikov, 2001; Pisanets et al., 2009), the precise taxonomic assignment of these remains is uncertain, so we conservatively used this information to place a minimum age for the TMRCA of all species in the group. We implemented this by setting a prior distribution for their TMRCA following a lognormal distribution with an offset of 9.7 Mya, and 95% of the values between 10.1 and 22.2 Mya. On the other hand, the oldest fossil remains confidently assigned to *B. verrucosissimus* are from the Pliocene of Russia (1.81–2.59 Mya), so we used this information to set a lognormal prior with an offset of 1.81 Mya and 95% of the values between 2 and 4.5 Mya. The birth–death process was specified for the tree prior, since it is well suited to a multispecies dataset with deep genetic divergence across clades and species. Four independent runs of 25 million generations, sampling every 2500 generations, were combined, after checking for convergence and adequate effective sample sizes (ESSs) of parameters of interest using the software Tracer (Rambaut and Drummond, 2007), to derive the median values and 95% highest posterior density intervals (HPDIs) of the corresponding TMRCAs.

Finally, we used the species tree reconstruction method implemented in ∗BEAST (Drummond and Rambaut, 2007; Heled and Drummond, 2010) to address phylogenetic relationships in the *B. bufo* species group. *Bufo gargarizans* was used as an outgroup. This analysis considered five independent partitions: 16S + cyt-b, POMC, CXCR4, BDNF and RPL3. For each of them, models of substitution were based on results of jModeltest. Clock rate and topology were unlinked in the five partitions. The birth–death process was chosen as the coalescent prior for the species tree. Three independent analyses were run for 50 million generations each, sampling every 5000 generations. Results were visualized in Tracer to check for convergence and adequate effective sample sizes (ESSs) of parameters.

3. Results

3.1. mtDNA

The mtDNA alignment contained 1239 sites across the 241 specimens studied (335 of them polymorphic), defining 123 haplotypes. Those more widespread and found at higher frequencies include haplotype 2 ($N = 11$), found in samples from the Netherlands, northern France, Germany, Belgium and Hungary (samples BB002, BB142, BB143, BB144, BB149, BB164, BB170, BB171, BB186, BB188, BB189); haplotype 6 ($N = 11$), in samples from southern France and north-eastern Spain (Pyrenees) (samples BB006, BB012, BB117, BB118, BB147, BB166, BB191, BB193, OBYX6, OBYX9 and OBYX19); and haplotype 9 ($N = 25$), in samples from Serbia, Hungary, Slovakia, Ukraine, Russia, and Romania (samples BB14, BB33, BB34, BB35, BB44, BB52, BB53, BB74, BB75, BB76, BB105, BB123, BB126, BB127, BB128, BB159, BB160, BB161, BB162, BB163, BB180, BB181, BB185, RO1, RO3) (Table 1). Phylogenetic analyses based on mtDNA data produced a well-resolved tree (Fig. 2A), with *B. eichwaldi* as the sister group of two clades (BPP = 1.0/MP bootstrap = 100/ML bootstrap = 100). Clade 1 (subsequently referred to as *Bufo spinosus*, see below) includes samples from North Africa, the Iberian Peninsula and France (1.0/100/100). *Bufo spinosus* is sister (1.0/97/100) to Clade 2 (1.0/100/100), which includes two subclades: one comprising samples from all other populations of *B. bufo,* from northern France to Siberia, including the Apennine peninsula and Sicily, the Balkan Peninsula and most of Anatolia (1.0/96/91), and another, weakly supported clade (<0.90/64/52), including all samples of *B. verrucosissimus.* At least three major subclades are recovered within *B. spinosus*: (1) samples from Morocco (1.0/100/100); (2) samples from Tunisia (1.0/100/99); and (3) samples from the Iberian Peninsula and most of France (1.0/100/100). Samples from Morocco and Tunisia are closely related to one another (1.0/100/99). Within *B. bufo* there are several well-supported clades, including: (1) southern Italy and Sicily (1.0/90/82); (2) the remaining samples from Italy (center and north) plus samples from the Balkans in Serbia, Montenegro, Albania, Macedonia and Greece (0.95/73/58); and (3) the remaining samples (1.0/84/79), including haplotypes found in the Balkans (Greece, Serbia, Montenegro), Anatolia, and also all samples from central, western and northern Europe (Germany, Netherlands, northern France, Belgium, Hungary, England, Poland, Russia, Ukraine, Sweden, Romania, Slovakia), which form a well-supported subclade (1.0/80/92) that includes additional samples from the Balkans (Serbia, Montenegro, Croatia) (Fig. 2A, Table 1). Finally, within *B. verrucosissimus* there are two well-supported subclades: one mainly distributed north of the Caucasus and comprising all samples from Russia plus one sample from Abkhazia, Georgia (BB059, Malaya Ritza lake) (1.0/80/73); and a second one including the remaining samples from southern Georgia and Turkey (0.99/94/91), south of the Caucasus. These groups do not reflect current subspecific assignments (Table 1), but rather allopatric groups of populations in the northwestern slopes of the Great Caucasus versus Lesser Caucasus and southern slope of the Great Caucasus, respectively (Fig. 1, Table 1).

Mean pairwise (*p*-uncorrected ± standard deviations) genetic distances between species are presented in Table 3 and range from 1.6 ± 0.3% (between *B. bufo* and *B. verrucosissimus*) to 7.7 ± 0.7% (between *B. spinosus* and *B eichwaldi*). Within *B. bufo* the mean uncorrected distance was 0.8 ± 0.1%; within *B. spinosus* it was 1.5 ± 0.1%, and within *B. eichwaldi* and *B. verrucosissimus*, 0.1 ± 0.07% and 0.2 ± 0.08%, respectively. The *B. bufo* clade included 171 individuals, with 98 variable sites defining 70 haplotypes (haplotype diversity, $h = 0.933$). Nucleotide diversity (π) was 0.008, and the average number of nucleotide differences (k) was 9.5. The *B. spinosus* clade included 43 individuals, with 102 variable sites defining 24 haplotypes, with similar values of haplotype diversity ($h = 0.910$) and higher nucleotide diversity ($\pi = 0.016$ and $k = 19.4$). The corresponding values for *B. eichwaldi* ($N = 5$) and *B. verrucosissimus* ($N = 13$) were, respectively, $h = 0.800$, $\pi = 0.001$ and $k = 1.4$; and $h = 0.692$, $\pi = 0.002$ and $k = 2.7$. Neutrality test results (Tajima's D, Fu and Li's D and F statistics) were not significant (results not shown).

Estimated TMRCAs (in Mya) for selected clades and subclades (median and 95% HPDIs) are as follows: *B. eichwaldi*: 0.19 (0.0364–0.53); *B. spinosus:* 5.18 (2.48–9.00); *B. bufo:* 1.70 (0.89–2.88); *B. bufo* + *B. verrucosissimus*: 2.75 (1.90–4.27); *B. spinosus* + *B. bufo* + *B. verrucosissimus*: 9.19 (5.37–15.76); *B. eichwaldi* + *B. spinosus* + *B. bufo* + *B. verrucosissimus*: 13.06 (9.81–21.83); *B. spinosus* (North Africa): 2.20 (0.81–4.23); *B. spinosus* (Iberia + France): 1.09 (0.50–2.05); *B. verrucosissimus* (NW Caucasus): 0.18 (0.0373–0.50); *B. verrucosissimus* (SW Caucasus): 0.11 (0.0079–0.36).

3.2. nDNA

The number of polymorphic sites in the nuclear markers was nine for POMC, nine for CXCR4, five for BDNF and 65 for RPL3. Results of neutrality (Tajima's D, Fu and Li's F and D) and recombination (PHI) tests were not significant (results not shown). Nuclear DNA topologies can be found in the Supplementary content section. In all cases, haplotypes grouped together according to species designations. For instance, haplotypes in *B. eichwaldi* were well differentiated from those found in the other species and always formed a monophyletic group. On the other hand, haplotypes in *B. spinosus* were also well differentiated: they were not found in other species and represent considerable diversity. Finally, haplotypes from *B. bufo* and *B. verrucosissimus* were closely related and in most cases formed well-supported clades (Supplementary content). The combined nDNA topology is consistent with these results and similar to the mtDNA tree (Fig. 2B), with *B. eichwaldi* sister to (*B. spinosus* + (*B. bufo* + *B. verrucosissimus*)) (1.0/100/100). *Bufo eichwaldi* (1.0/89/91) and *B. spinosus* (1.0/84/89) were recovered as monophyletic groups. A sister group between *B. spinosus* and (*B. bufo* + *B. verrucosissimus*) was also well supported (1.0/89/86). Samples of *B. verrucosissimus* were nested within *B. bufo* (Fig. 2B) and were most similar to samples of *B. bufo* from Turkey (BB070) and Greece (BB117), with which they form a subclade (0.99/–/52) that, in turn, includes another subclade with samples from central and southern Italy and Sicily (OGAM2, OMON5, ORAG3, 5, see Table 1 and Fig. 1) (1.0/–/76).

3.3. Combined mtDNA + nDNA analyses

The combined mtDNA + nDNA topology (Fig. 3A) is very similar to the mtDNA tree, with *B. eichwaldi* as sister to (*B. spinosus* + (*B. verrucosissimus* + *B. bufo*)), with BPPs = 1.0 and bootstrap values = 100 in all cases. However, whereas the monophyly of *B. eichwaldi* (1.0/100/100), *B. spinosus* (1.0/100/100) and *B. verrucosissimus* (1.0/76/82) is also well supported, the monophyly of *B. bufo* is well supported in MP (88) but not in ML (where *B. verrucosissimus* is nested within *B. bufo*) or Bayesian (<0.9) analyses (Fig. 3A). On the other hand, results of *BEAST analyses produced a fully resolved topology, with *B. eichwaldi* sister to (*B. spinosus* (*B. bufo* + *B. verrucosissimus*)), with all nodes having BPPs > 0.95 (Fig. 3B).

4. Discussion

Our combination of comprehensive geographic sampling and choice of molecular markers with different substitution rates and patterns of inheritance has produced a fully resolved phylogenetic hypothesis for Eurasian and north African species in the *B. bufo* species group. Our results indicate an old (Miocene) origin for the current species diversity in the group, with the initial split of the ancestors of *B. eichwaldi* in the Caucasus, and of *B. bufo* (*sensu lato*) in the western Mediterranean region around 9–13 Mya. The congruence between the results of analyses based on mtDNA, nDNA, concatenated analyses of mitochondrial and nuclear DNA,

Table 1
Sampling localities: species, sample codes, latitude, longitude, and GenBank Accession numbers for the sequences generated in this study.

Species	Sample code	Country	Locality	Latitude	Longitude	mtDNA haplotype	16S	cytb	POMC	CXCR4	BDNF	RPL3
Bufo bufo	BB194	Albania	Near Tepelena	40°17′25.20″N	20°01′30.30″E	25	JN647155	JN647341				
Bufo bufo	BB188	Belgium	Liege prov: Solwaster	50°31′23.00″N	5°58′32.00″E	2	JN647153	JN647339				
Bufo bufo	BB189	Belgium	Liege prov: Marche-en-Famenne	50°15′49.00″N	5°22′7.00″E	2	JN647154	JN647340				
Bufo bufo	BB157	Croatia	Svika	44°52′20.73″N	15°10′56.39″E	17	JN647136	JN647319				
Bufo bufo	BB158	Croatia	Zutica	45°37′51.68″N	16°26′43.62″E	77	JN647137	JN647320				
Bufo bufo	BB141	France	Erloy, Foret de Regnaval	49°54′60.00″N	3°50′30.00″E	71	JN647129	JN647313	JN646935	JN646884	JN646979	JN647505
Bufo bufo	BB142	France	Bruyéres et Montbérault	49°32′6.00″N	3°40′40.00″E	2	JN647130	JN647314				
Bufo bufo	BB143	France	Le Boujon	49°56′55.00″N	3°50′15.00″E	2	JN647131	JN647315				
Bufo bufo	BB144	France	Le Chevalet	50°1′0.00″N	3°52′30.00″E	2	JN647132	JN647316				
Bufo bufo	BB145	France	Nouvion	50°0′20.00″N	3°46′45.00″E	23	JN647133	JN647317				
Bufo bufo	BB146	France	Vorges	49°31′0.84″N	3°38′49.08″E	23	JN647134	JN647318				
Bufo bufo	BB149	France	Chigny	49°17′57.75″N	3°46′30.00″E	2	JN647135	JN647329				
Bufo bufo	BB164	France	Audresselles, dept. Pas-de-Calais	50°49′16.10″N	1°36′8.30″E	2	JN647143	JN647326				
Bufo bufo	OBYX12	France	Saint Bonnet en Champsaur	44°40′58.42″N	6°4′34.13″E	106	JN647224	JN647419				
Bufo bufo	BB001	Germany	Eberswalde, Bad Freienwald, ~50 km NE Berlin	52°49′32.52″N	13°48′58.32″E	1	JN647011	JN647247				
Bufo bufo	BB170	Germany	Bonn, W Rhine	50°41′52.00″N	7°7′42.00″E	2	JN647147	JN647333				
Bufo bufo	BB171	Germany	Bonn, W Rhine	50°41′52.00″N	7°7′42.00″E	2	JN647148	JN647334				
Bufo bufo	BB026	Greece	3 km W Nea Zoi	39°43′28.40″N	21°45′14.44″E	20	JN647026	JN647262				
Bufo bufo	BB107	Greece	Thessalia, Desi	39°33′37.51″N	21°22′18.70″E	54	JN647117	JN647301	JN646932	JN646881	JN646977	JN647503
Bufo bufo	BB108	Greece	Thessalia, Desi	39°33′37.51″N	21°22′18.70″E	55	JN647118	JN647302				
Bufo bufo	BB109	Greece	Thraki, Sofiko	41°26′21.95″N	26°36′30.96″E	56	JN647119	JN647303				
Bufo bufo	BB111	Greece	Makedonia, Lepida timberyard	41°23′22.52″N	24°38′15.43″E	57	JN647120	JN647304				
Bufo bufo	BB112	Greece	Makedonia, Lepida timberyard	41°23′22.52″N	24°38′15.43″E	58	JN647121	JN647305				
Bufo bufo	BB114	Greece	Sterea Ellada, Gkiona mt., at stream by Agios Nikolaos church, on the road from Ptrosilio to Amfissa	38°33′51.77″N	22°20′56.69″E	59	JN647122	JN647306	JN646933	JN646882	JN646978	
Bufo bufo	BB032	Hungary	Öcs	47°0′34.10″N	17°37′49.21″E	23	JN647032	JN647268				
Bufo bufo	BB033	Hungary	Öcs	47°0′34.10″N	17°37′49.21″E	9	JN647033	JN647269				
Bufo bufo	BB034	Hungary	Pécs, Jakab-Hill, Mecsek Mts.	46°5′35.34″N	18°8′28.98″E	9	JN647034	JN647270				
Bufo bufo	BB179	Hungary	Vinye, Bakony Mts.	47°21′11.28″N	17°46′44.64″E	88	JN647158	JN647344	JN646930	JN646886	JN646988	JN647492
Bufo bufo	BB180	Hungary	Erdőbénye, Zemplén Mts.	48°18′50.70″N	21°20′4.96″E	9	JN647159	JN647345	JN646931	JN646887	JN646981	JN647493
Bufo bufo	BB181	Hungary	Bakonybél, Bakony Mts.	47°16′7.38″N	17°41′41.28″E	9	JN647160	JN647346				
Bufo bufo	BB182	Hungary	Szendrő	48°23′44.88″N	20°44′27.84″E	89	JN647161	JN647347				
Bufo bufo	BB183	Hungary	Csákánydoroszló	46°58′1.50″N	16°30′29.40″E	88	JN647162	JN647348				
Bufo bufo	BB184	Hungary	Őrség, Bárkás-lake	46°53′59.40″N	16°27′53.29″E	90	JN647163	JN647349				
Bufo bufo	BB185	Hungary	Tihany	46°54′33.12″N	17°50′57.26″E	9	JN647164	JN647350				
Bufo bufo	BB186	Hungary	Bátaapáti	46°12′54.12″N	18°36′41.25″E	2	JN647165	JN647351				
Bufo bufo	BB187	Hungary	Bátaapáti	46°12′54.12″N	18°36′41.25″E	91	JN647166	JN647352				
Bufo bufo	OALB4	Italy	Alberobello	40°47′10.59″N	17°14′14.84″E	100	JN647175	JN647361				
Bufo bufo	OANG10	Italy	Lago dell’ Antigola	38°44′22.41″N	16°14′9.51″E	101	JN647176	JN647362				
Bufo bufo	OANG8	Italy	Lago dell’ Antigola	38°44′22.41″N	16°14′9.51″E	102	JN647177	JN647363				
Bufo bufo	OBEL2	Italy	Bel Monte Calabro Marina	39°10′2.52″N	16°4′44.87″E	103	JN647178	JN647364				
Bufo bufo	OBRB15	Italy	Barbarano	42°16′11.63″N	12°3′38.28″E	104	JN647179	JN647365				
Bufo bufo	OBRB2	Italy	Barbarano	42°16′11.63″N	12°3′38.28″E	104	JN647180	JN647366				
Bufo bufo	ODOG10	Italy	Doganella	41°45′00.35″N	12°45′39.60″E	107	JN647054	JN647367				
Bufo bufo	ODOG5	Italy	Doganella	41°45′00.35″N	12°45′39.60″E	107	JN647055	JN647368				
Bufo bufo	ODOG8	Italy	Doganella	41°45′00.35″N	12°45′39.60″E	107	JN647056	JN647369				
Bufo bufo	ODOG9	Italy	Doganella	41°45′00.35″N	12°45′39.60″E	107	JN647057	JN647370				
Bufo bufo	OFAG2	Italy	Fagnano Castello-Lago Paglia	39°33′57.59″N	16°3′15.42″E	108	JN647058	JN647371				
Bufo bufo	OFAG5	Italy	Fagnano Castello-Lago Paglia	39°33′57.59″N	16°3′15.42″E	109	JN647059	JN647372				
Bufo bufo	OFIUB1	Italy	Fiumefreddo Bruzio	39°15′28.62″N	16°5′44.61″E	103	JN647060	JN647373				
Bufo bufo	OFIUB2	Italy	Fiumefreddo Bruzio	39°15′28.62″N	16°5′44.61″E	103	JN647061	JN647374	JN646917	JN646869		JN647483
Bufo bufo	OFIUB3	Italy	Fiumefreddo Bruzio	39°15′28.62″N	16°5′44.61″E	103	JN647062	JN647375	JN646918			

(*continued on next page*)

Table 1 (*continued*)

Species	Sample code	Country	Locality	Latitude	Longitude	mtDNA haplotype	16S	cytb	POMC	CXCR4	BDNF	RPL3
Bufo bufo	OFIUB4	Italy	Fiumefreddo Bruzio	39°15′28.62″N	16°5′44.61″E	103	JN647063	JN647376				
Bufo bufo	OFOG4	Italy	Bosco del Foglino	41°28′14.95″N	12°43′6.02″E	110	JN647064	JN647377				
Bufo bufo	OFOG5	Italy	Bosco del Foglino	41°28′14.95″N	12°43′6.02″E	107	JN647065	JN647378				
Bufo bufo	OFOG9	Italy	Bosco del Foglino	41°28′14.95″N	12°43′6.02″E	111	JN647066	JN647379				
Bufo bufo	OGAM2	Italy	Gambarie	38°10′51.59″N	15°50′45.32″E	101	JN647068	JN647381	JN646919	JN646870	JN646967	JN647485
Bufo bufo	OGAM22	Italy	Gambarie	38°10′51.59″N	15°50′45.32″E	112	JN647067	JN647380	JN646920	JN646871	JN646968	
Bufo bufo	OGHI2	Italy	Monghidoro	44°14′53.89″N	11°20′46.43″E	107	JN647069	JN647382		JN646872	JN646969	JN647484
Bufo bufo	OGHI4	Italy	Monghidoro	44°14′53.89″N	11°20′46.43″E	107	JN647070	JN647383				
Bufo bufo	OJEN1	Italy	Jenne	41°53′23.47″N	13°10′14.33″E	113	JN647071	JN647384	JN646921	JN646873		JN647486
Bufo bufo	OJEN2	Italy	Jenne	41°53′23.47″N	13°10′14.33″E	107	JN647072	JN647385				
Bufo bufo	OJEN3	Italy	Jenne	41°53′23.47″N	13°10′14.33″E	114	JN647073	JN647386				
Bufo bufo	OMAS2	Italy	Tortora -C.da Massadita-	39°56′30.93″N	15°48′21.54″E	115	JN647074	JN647387				
Bufo bufo	OMAS3	Italy	Tortora -C.da Massadita-	39°56′30.93″N	15°48′21.54″E	116	JN647075	JN647388				
Bufo bufo	OMAS4	Italy	Tortora -C.da Massadita-	39°56′30.93″N	15°48′21.54″E	100	JN647076	JN647389				
Bufo bufo	OMAS5	Italy	Tortora -C.da Massadita-	39°56′30.93″N	15°48′21.54″E	100	JN647077	JN647390				
Bufo bufo	OMOL1	Italy	Molella- Fonti di Locullo	41°16′5.09″N	13°2′44.20″E	107	JN647078	JN647391				
Bufo bufo	OMOL2	Italy	Molella- Fonti di Locullo	41°16′5.09″N	13°2′44.20″E	107	JN647079	JN647392				
Bufo bufo	OMOL4	Italy	Molella- Fonti di Locullo	41°16′5.09″N	13°2′44.20″E	117	JN647080	JN647393				
Bufo bufo	OMOL6	Italy	Molella- Fonti di Locullo	41°16′5.09″N	13°2′44.20″E	107	JN647081	JN647394				
Bufo bufo	OMON1	Italy	Canale Monterano	42°8′25.68″N	12°5′49.46″E	107	JN647083	JN647396	JN646922	JN646874	JN646970	
Bufo bufo	OMON16	Italy	Canale Monterano	42°8′25.68″N	12°5′49.46″E	107	JN647082	JN647395				
Bufo bufo	OMON4	Italy	Canale Monterano	42°8′25.68″N	12°5′49.46″E	118	JN647084	JN647397	JN646923	JN646875	JN646971	
Bufo bufo	OMON5	Italy	Canale Monterano	42°8′25.68″N	12°5′49.46″E	107	JN647085	JN647398	JN646924	JN646876	JN646972	JN647487
Bufo bufo	OORS10	Italy	Orsomarso	39°48′1.37″N	15°54′28.58″E	100	JN647086	JN647399				
Bufo bufo	OORS2	Italy	Orsomarso	39°48′1.37″N	15°54′28.58″E	100	JN647087	JN647400				
Bufo bufo	OORS6	Italy	Orsomarso	39°48′1.37″N	15°54′28.58″E	100	JN647088	JN647401				
Bufo bufo	ORAG3	Italy	Fiume Irminio	36°55′44.01″N	14°40′25.03″E	101	JN647089	JN647402	JN646925	JN646877	JN646973	JN647488
Bufo bufo	ORAG5	Italy	Fiume Irminio	36°55′44.01″N	14°40′25.03″E	119	JN647090	JN647403	JN646926	JN646878	JN646974	JN647489
Bufo bufo	ORAG8	Italy	Fiume Irminio	36°55′44.01″N	14°40′25.03″E	119	JN647091	JN647404	JN646927	JN646879	JN646975	
Bufo bufo	ORAG9	Italy	Fiume Irminio	36°55′44.01″N	14°40′25.03″E	101	JN647092	JN647405		JN646880	JN646976	JN647490
Bufo bufo	OSTI1	Italy	Stilo	38°28′41.27″N	16°28′9.20″E	101	JN647093	JN647406				
Bufo bufo	OSUB2	Italy	Subiaco	41°50′28.12″N	13°2′20.36″E	120	JN647094	JN647407				
Bufo bufo	OSUB5	Italy	Subiaco	41°50′28.12″N	13°2′20.36″E	107	JN647095	JN647408				
Bufo bufo	OTIZ2	Italy	Campo Tizzoro	44°2′19.22″N	10°51′42.19″E	121	JN647096	JN647409				
Bufo bufo	OTIZ3	Italy	Campo Tizzoro	44°2′19.22″N	10°51′42.19″E	122	JN647097	JN647410				
Bufo bufo	OTIZ5	Italy	Campo Tizzoro	44°2′19.22″N	10°51′42.19″E	122	JN647098	JN647411				
Bufo bufo	OTUR3	Italy	Rocca Sinibalda-fiume Turano	42°16′29.47″N	12°55′32.25″E	107	JN647099	JN647412				
Bufo bufo	OTUR4	Italy	Rocca Sinibalda-fiume Turano	42°16′29.47″N	12°55′32.25″E	107	JN647100	JN647413				
Bufo bufo	OTUR5	Italy	Rocca Sinibalda-fiume Turano	42°16′29.47″N	12°55′32.25″E	107	JN647101	JN647414				
Bufo bufo	OVER1	Italy	Piani di Verteglia	41°1′10.64″N	15°0′23.11″E	100	JN647102	JN647415				
Bufo bufo	OVER2	Italy	Piani di Verteglia	41°1′10.64″N	15°0′23.11″E	123	JN647103	JN647416				
Bufo bufo	OVER3	Italy	Piani di Verteglia	41°1′10.64″N	15°0′23.11″E	100	JN647104	JN647417				
Bufo bufo	OVER4	Italy	Piani di Verteglia	41°1′10.64″N	15°0′23.11″E	100	JN647105	JN647418				
Bufo bufo	BB196	Macedonia	Prilep – Dunje	41°20′13.00″N	21°42′1.50″E	25	JN647157	JN647343				
Bufo bufo	BB019	Montenegro	Bjelasica mt-Biogradsko jezero	42°54′5.60″N	19°35′49.20″E	14	JN647019	JN647255				
Bufo bufo	BB029	Montenegro	Bjelasica mt-Dolovi	42°53′55.20″N	19°38′1.80″E	21	JN647029	JN647265				
Bufo bufo	BB030	Montenegro	Bjelasica mt-Svatovsko Groblje	42°53′46.80″N	19°38′38.16″E	22	JN647030	JN647266				
Bufo bufo	BB195	Montenegro	Bjelosi	42°22′10.40″N	18°53′26.60″E	25	JN647156	JN647342				
Bufo bufo	BB002	Netherlands	Elspeet	52°18′15.35″N	5°49′31.22″E	2	JN647012	JN647248	JN646916	JN646866	JN646964	JN647500
Bufo bufo	BB174	Poland	Zgorzelec	51°8′12.70″N	15°1′3.80″E	82	JN647149	JN647335				
Bufo bufo	BB176	Poland	Stara Wies	51°47′20.76″N	15°43′41.52″E	83	JN647150	JN647336				
Bufo bufo	BB177	Poland	Szubin	53°0′5.35″N	17°44′13.26″E	84	JN647151	JN647337				
Bufo bufo	BB178	Poland	Wroclen – Pruszowice	50°12′0.46″N	20°47′37.76″E	85	JN647152	JN647338				
Bufo bufo	BB105	Romania	Măcin Mountains National Park	45°13′59.90″N	28°18′31.30″E	9	JN647116	JN647300				
Bufo bufo	BB122	Romania	Călăraşi-Chiciu	44°51′48.60″N	27°52′33.24″E	13	JN647123	JN647307				

Bufo bufo	BB123	Romania	Coşnea	47°52′0.85″N	24°30′55.44″E	9	JN647124	JN647308				
Bufo bufo	BB125	Romania	Insula Mică a Brăilei	44°51′48.60″N	27°52′33.24″E	64	JN647125	JN647309				
Bufo bufo	BB126	Romania	Lacul Roşu	46°46′57.72″N	25°47′1.68″E	9	JN647126	JN647310				
Bufo bufo	BB127	Romania	Motru Sec Cloşani	45°7′36.48″N	22°48′29.52″E	9	JN647127	JN647311				
Bufo bufo	BB128	Romania	Vidraru Reservoir, Făgăraş Mts.	45°26′32.65″N	24°36′21.96″E	9	JN647128	JN647312	JN646934	JN646883	JN646963	JN647504
Bufo bufo	BBUINSULA_B	Romania	Insula Mică a Brăilei	44°51′48.60″N	27°52′33.24″E	18	JN647171	JN647357				
Bufo bufo	RO1	Romania	Luncaviţa	45°14′20.51″N	28°17′49.19″E	9	JN647168	JN647354				
Bufo bufo	RO2	Romania	Luncaviţa	45°14′20.51″N	28°17′49.19″E	96	JN647169	JN647355				
Bufo bufo	RO3	Romania	Luncaviţa	45°14′20.51″N	28°17′49.19″E	9	JN647170	JN647356				
Bufo bufo	BB053	Russia	Moscow province, Zvenigorod	55°42′39.20″N	36°46′16.40″E	9	JN647050	JN647286				
Bufo bufo	BB054	Russia	Krasnoyarsk territory, Mirnyi	62°16′55.50″N	89°2′2.20″E	31	JN647051	JN647287				
Bufo bufo	BB055	Russia	Sverdlovsk prov., Ekaterinburg	56°50′25.40″N	60°33′20.30″E	31	JN647052	JN647288	JN646939	JN646890	JN646984	JN647496
Bufo bufo	BB056	Russia	Novosibirsk prov., Novosibirsk	55°3′41.30″N	82°52′31.40″E	31	JN647053	JN647289				
Bufo bufo	BB074	Russia	Tver province, Toropets	56°31′48.00″N	31°32′6.50″E	9	JN647108	JN647292				
Bufo bufo	BB075	Russia	Yaroslavl province, Yaroslavl	57°35′54.50″N	39°53′17.40″E	9	JN647109	JN647293				
Bufo bufo	BB076	Russia	Orel province, Orlovskiye Zaseki NP	53°20′57.50″N	35°33′30.50″E	9	JN647110	JN647294		JN646892		JN647498
Bufo bufo	BB077	Russia	Krasnoyarsk territory, Kryuchkovo	56°5′42.50″N	92°8′10.50″E	38	JN647111	JN647295			JN646986	
Bufo bufo	BB079	Russia	Karelia, Kindo peninsula	66°32′8.40″N	33°9′41.00″E	39	JN647112	JN647296				
Bufo bufo	BB080	Russia	Arkhangelsk province, Arkhangelsk environs	64°32′39.50″N	40°41′22.50″E	39	JN647113	JN647297	JN646941	JN646893	JN646987	JN647499
Bufo bufo	BB081	Russia	Tatarstan, Kazan environs	55°52′9.30″N	49°8′40.60″E	39	JN647114	JN647298				
Bufo bufo	BB014	Serbia	Avala mt – Tresnja	44°36′26.60″N	20°34′14.00″E	9	JN647014	JN647250				
Bufo bufo	BB015	Serbia	Avala mt – Tresnja	44°36′26.60″N	20°34′14.00″E	10	JN647015	JN647251				
Bufo bufo	BB016	Serbia	Avala mt – Zuce	44°40′55.90″N	20°33′55.90″E	11	JN647016	JN647252				
Bufo bufo	BB017	Serbia	Avala mt – Zuce	44°40′55.90″N	20°33′55.90″E	12	JN647017	JN647253	JN646936	JN646885	JN646980	JN647491
Bufo bufo	BB018	Serbia	Avala mt – Zuce	44°40′55.90″N	20°33′55.90″E	13	JN647018	JN647254				
Bufo bufo	BB020	Serbia	Pozega-Rupeljevo 1	43°46′44.58″N	19°59′49.74″E	15	JN647020	JN647256				
Bufo bufo	BB021	Serbia	Pozega-Rupeljevo 1	43°46′44.58″N	19°59′49.74″E	15	JN647021	JN647257				
Bufo bufo	BB022	Serbia	Pozega-Rupeljevo 1	43°46′44.58″N	19°59′49.74″E	16	JN647022	JN647258				
Bufo bufo	BB023	Serbia	Pozega-Rupeljevo 2	43°46′48.30″N	19°59′21.90″E	17	JN647023	JN647259				
Bufo bufo	BB024	Serbia	Pozega-Rupeljevo 2	43°46′48.30″N	19°59′21.90″E	18	JN647024	JN647260				
Bufo bufo	BB025	Serbia	Valjevo-Petnica	44°14′50.00″N	19°55′51.00″E	19	JN647025	JN647261				
Bufo bufo	BB027	Serbia	Leskovac-Pasina Cesma	43°2′36.30″N	21°52′10.20″E	14	JN647027	JN647263				
Bufo bufo	BB028	Serbia	Golija mt-Devici	43°25′18.84″N	20°22′47.16″E	15	JN647028	JN647264				
Bufo bufo	BB031	Serbia	Avala mt – Tresnja	44°36′26.60″N	20°34′14.00″E	21	JN647031	JN647267				
Bufo bufo	BB038	Serbia	Vranje – Bustranje (1)	42°26′3.00″N	21°54′13.00″E	17	JN647037	JN647273				
Bufo bufo	BB039	Serbia	Vranje – Bustranje (2)	42°25′60.00″N	21°54′17.00″E	17	JN647038	JN647274				
Bufo bufo	BB040	Serbia	Vranje-Rusce	42°24′50.00″N	21°56′48.00″E	13	JN647039	JN647275				
Bufo bufo	BB041	Serbia	Vranje-Gornje Zupsko	42°27′3.00″N	21°53′21.00″E	25	JN647040	JN647276				
Bufo bufo	BB042	Serbia	Bosilegrad	42°29′58.40″N	22°28′23.30″E	25	JN647041	JN647277				
Bufo bufo	BB043	Serbia	Pozega-Rupeljevo 1	43°46′44.58″N	19°59′49.74″E	15	JN647042	JN647278				
Bufo bufo	BB036	Serbia-Kosovo	Novo Brdo-Prekovce	42°36′58.00″N	21°26′6.40″E	24	JN647036	JN647272	JN646937	JN646888	JN646982	JN647494
Bufo bufo	BB035	Slovakia	Bratislava – Zelezna studnicka	48°10′60.00″N	17°4′60.00″E	9	JN647035	JN647271				
Bufo bufo	BB044	Slovakia	Donovaly	48°52′0.00″N	19°13′60.00″E	9	JN647043	JN647279				
Bufo bufo	BBUSLO5	Slovakia	Sastin-Straze	48°37′60.00″N	17°7′60.00″E	92	JN647167	JN647353				
Bufo bufo	BB046	Sweden	Umea – Frederika	64°5′59.99″N	18°22′59.88″E	26	JN647044	JN647280	JN646938	JN646889	JN646983	JN647495
Bufo bufo	BB048	Sweden	Skane-Stensoffa (Lund)	55°40′59.88″N	13°26′60.00″E	27	JN647045	JN647281				
Bufo bufo	BB049	Sweden	Umea – Frederika	64°5′59.99″N	18°22′59.88″E	28	JN647046	JN647282				
Bufo bufo	BB050	Sweden	Skane-Stensoffa (Lund)	55°40′59.88″N	13°26′60.00″E	29	JN647047	JN647283				
Bufo bufo	BB051	Sweden	Umea – Frederika	64°5′59.99″N	18°22′59.88″E	30	JN647048	JN647284				
Bufo bufo	BB167	Sweden	Vastra Götaland, Göteborg,Slätta damm	57°43′60.00″N	11°55′0.00″E	79	JN647144	JN647330				
Bufo bufo	BB168	Sweden	Vastra Götaland, Göteborg,Slätta damm	57°43′60.00″N	11°55′0.00″E	80	JN647145	JN647331				
Bufo bufo	BB169	Sweden	Vastra Götaland, Göteborg,Slätta damm	57°43′60.00″N	11°55′0.00″E	81	JN647146	JN647332				
Bufo bufo	BB070	Turkey	Belalankoyu – Havza	41°10′50.50″N	35°46′26.60″E	36	JN647106	JN647290	JN646940	JN646891	JN646985	JN647497
Bufo bufo	BB071	Turkey	Erbaa	40°49′41.40″N	36°36′5.80″E	37	JN647107	JN647291				
Bufo bufo	BBUTURK2A	Turkey	Kiriklar-Eflani (loc. 2)	41°23′27.90″N	32°49′3.80″E	97	JN647172	JN647358				
Bufo bufo	BBUTURK3A	Turkey	Belalankoyu – Havza	41°10′50.50″N	35°46′26.60″E	98	JN647173	JN647359				
Bufo bufo	BBUTURK4A	Turkey	Erbaa	40°49′41.40″N	36°36′5.80″E	99	JN647174	JN647360				
Bufo bufo	BB004	UK	Wymeswold ″C″	52°48′20.00″N	1°6′24.00″W	4	JN647013	JN647249	JN646928	JN646867	JN646965	JN647501

(*continued on next page*)

Table 1 (*continued*)

Species	Sample code	Country	Locality	Latitude	Longitude	mtDNA haplotype	16S	cytb	POMC	CXCR4	BDNF	RPL3
Bufo bufo	BB008	UK	Holly Hayes	52°40′17.00″N	1°6′52.00″W	-	JN653289	-	JN646929	JN646868	JN646966	JN647502
Bufo bufo	BB052	Ukraine	Zakarpatska prov., Perechin district, Polonina Runa	48°47′21.00″N	22°47′51.50″E	9	JN647049	JN647285				
Bufo bufo	BB092	Ukraine	Zakarpatska prov., Perechin district, Lumshory environs	48°48′36.50″N	22°45′10.30″E	45	JN647115	JN647299				
Bufo bufo	BB159	Ukraine	Iskiv pond	49°37′33.97″N	36°17′7.89″E	9	JN647138	JN647321				
Bufo bufo	BB160	Ukraine	Iskiv pond	49°37′33.97″N	36°17′7.89″E	9	JN647139	JN647322				
Bufo bufo	BB161	Ukraine	Koryakin pond	49°37′10.94″N	36°18′50.04″E	9	JN647140	JN647323				
Bufo bufo	BB162	Ukraine	Koryakin pond	49°37′10.94″N	36°18′50.04″E	9	JN647141	JN647324				
Bufo bufo	BB163	Ukraine	Koryakin pond	49°37′10.94″N	36°18′50.04″E	9	JN647142	JN647325				
Bufo eichwaldi	BB062	Azerbaijan	Lerik district, Agoshapeshta env., Talysh mts.	38°39′34.20″N	48°38′9.30″E	34	JN647240	JN647476	JN646953	JN646908	JN647002	
Bufo eichwaldi	BB084	Azerbaijan	Astara district, Kizhaba environs, Talysh mts.	38°33′55.50″N	48°47′51.50″E	41	JN647239	JN647475	JN646955	JN646906	JN647003	JN647518
Bufo eichwaldi	BB086	Azerbaijan	Lerik district, Tankevan, Shovu and Zarikiumandjo environs, Talysh mts.	38°41′44.50″N	48°35′22.30″E	42	JN647241	JN647474	JN646954	JN646909	JN647005	
Bufo eichwaldi	BB091	Azerbaijan	Lerik district, Agoshapeshta env., Talysh mts.	38°39′34.20″N	48°38′9.30″E	44	JN647238	JN647477				
Bufo eichwaldi	BB140	Azerbaijan	Astara district, Kizhaba environs, Talysh mts.	38°33′55.50″N	48°47′51.50″E	70	JN647242	JN647478		JN646907	JN647004	
Bufo spinosus	BB005	France	Beauzelle	43°39′56.70″N	1°23′39.50″E	5	JN647219	JN647420	JN646943	JN646895	JN646990	JN647507
Bufo spinosus	BB006	France	Mount Canigou	42°33′56.20″N	2°25′11.00″E	6	JN647220	JN647421				
Bufo spinosus	BB116	France	Juigny	46°58′24.95″N	0°19′50.56″W	60	JN647212	JN647426				
Bufo spinosus	BB117	France	Embrun	44°33′18.72″N	6°30′26.50″E	6	JN647213	JN647427		JN646897	JN646992	JN647509
Bufo spinosus	BB118	France	La Manouesse	43°29′17.88″N	5°26′3.08″E	6	JN647214	JN647428	JN646945	JN646898	JN647001	JN647510
Bufo spinosus	BB132	France	French Pyrenees (near Arguenos)	42°58′14.48″N	0°43′26.29″E	67	JN647207	JN647435				
Bufo spinosus	BB147	France	Fougerolles de Plessis	48°28′31.70″N	0°58′5.10″W	6	JN647197	JN647327				
Bufo spinosus	BB148	France	St. Mars sur la Futane	48°25′56.10″N	1°1′4.60″W	72	JN647198	JN647328				
Bufo spinosus	BB165	France	St Pierre des Nids near Pre-en-Pail, dept. Mayenne	48°23′54.57″N	0°6′0.82″W	78	JN647195	JN647445				
Bufo spinosus	BB166	France	In between Vautorte and St Denis de Gastines, dept. Mayenne	48°18′42.00″N	0°50′40.08″W	6	JN647196	JN647446				
Bufo spinosus	BB190	France	Moulin ouest	43°53′20.23″N	3°23′50.39″E	86	JN647191	JN647447				
Bufo spinosus	BB191	France	Bergerie Hôpital	43°51′38.06″N	3°22′44.75″E	6	JN647192	JN647448				
Bufo spinosus	BB192	France	Sorbs (Ville Vieille)	43°53′56.04″N	3°24′19.81″E	87	JN647193	JN647449				
Bufo spinosus	BB193	France	Sotch de Caylus	43°53′21.11″N	3°23′13.24″E	6	JN647194	JN647450				
Bufo spinosus	OBYX19	France	Saint Bonnet en Champsaur	44°40′58.42″N	6°4′34.13″E	6	JN647181	JN647457				
Bufo spinosus	OBYX6	France	Saint Bonnet en Champsaur	44°40′58.42″N	6°4′34.13″E	6	JN647182	JN647458				
Bufo spinosus	OBYX8	France	Saint Bonnet en Champsaur	44°40′58.42″N	6°4′34.13″E	105	JN647183	JN647459				
Bufo spinosus	OBYX9	France	Saint Bonnet en Champsaur	44°40′58.42″N	6°4′34.13″E	6	JN647184	JN647460				
Bufo spinosus	BB119	Morocco	Ifrane	33°31′51.74″N	5°6′19.58″W	61	JN647215	JN647429	JN646946	JN646899	JN646993	JN647511
Bufo spinosus	BB120	Morocco	Ifrane	33°31′51.74″N	5°6′19.58″W	62	JN647216	JN647430	JN646948	JN646900	JN646995	JN647512
Bufo spinosus	BB121	Portugal	Portalegre	39°19′52.68″N	7°19′23.81″W	63	JN647217	JN647431	JN646949	JN646901	JN646996	
Bufo spinosus	BB150	Portugal	Portalegre	39°19′52.68″N	7°19′23.81″W	73	JN647199	JN647440			JN646998	JN647515
Bufo spinosus	BB003	Spain	35 km NE Capileira	36°58′26.20″N	3°19′21.30″W	3	JN647218	JN647425	JN646942	JN646894	JN646989	JN647506
Bufo spinosus	BB010	Spain	A Pobra do Caramiñal	42°36′26.01″N	8°57′39.18″W	7	JN647221	JN647422	JN646944	JN646905	JN646991	JN647508
Bufo spinosus	BB012	Spain	Sadernes	42°16′43.30″N	2°35′24.60″E	6	JN647222	JN647423	JN646947	JN646896	JN646994	JN647513
Bufo spinosus	BB013	Spain	Laguna Grande de Gredos	40°15′11.00″N	5°16′33.00″W	8	JN647223	JN647424	JN646950	JN646902	JN646997	JN647514
Bufo spinosus	BB129	Spain	Plá dels Corrals (Simat de la Valldigna)	39°2′36.77″N	0°18′38.16″W	65	JN647204	JN647432				
Bufo spinosus	BB130	Spain	A Coruña	43°22′17.37″N	8°23′45.49″W	60	JN647205	JN647433				
Bufo spinosus	BB131	Spain	Laguna de los Peces (Parque de Sanabria). San Martín de los Gallegos	42°10′26.91″N	6°43′47.73″W	66	JN647206	JN647434				
Bufo spinosus	BB133	Spain	Majaelrayo a Cantalojas	41°9′39.70″N	3°18′53.90″W	68	JN647208	JN647436				
Bufo spinosus	BB134	Spain	Hecho	42°44′11.10″N	0°45′37.40″W	69	JN647209	JN647437				
Bufo spinosus	BB135	Spain	Fanlo a Escalona	42°35′15.40″N	0°0′47.30″W	60	JN647210	JN647438				
Bufo spinosus	BB137	Spain	Laújar	37°5′6.60″N	2°54′17.00″W	3	JN647211	JN647439				
Bufo spinosus	MNCN_10071	Spain	Pelahustán. Carretera de Cenicientos	40°10′34.56″N	4°35′48.97″W	93	JN647186	JN647452				
Bufo spinosus	MNCN_15574	Spain	San Esteve ses Rovires	41°29′40.38″N	1°52′22.08″E	94	JN647187	JN647453				
Bufo spinosus	MNCN_15581	Spain	Lago Enol. Covadonga	43°16′20.68″N	4°59′28.21″W	60	JN647188	JN647454				
Bufo spinosus	MNCN_15600	Spain	Mougás, Pontevedra	42°3′4.46″N	8°52′21.41″W	95	JN647189	JN647455				
Bufo spinosus	MNCN_15622	Spain	Río Madera. Orcera	38°19′2.58″N	2°39′53.68″W	3	JN647190	JN647456				
Bufo spinosus	MNCN_8003	Spain	Valdemanco	40°52′21.09″N	3°39′46.64″W	93	JN647185	JN647451				
Bufo spinosus	BB152	Tunisia	Beni M'Tir (loc. 2)	36°44′13.30″N	8°43′3.70″E	74	JN647200	JN647441	JN646951	JN646903	JN646999	JN647516

Bufo spinosus	BB153	Tunisia	Beni M'Tir (loc. 4)	36°44′27.10″N	8°42′54.30″E	75	JN647201	JN647442	JN646952	JN646904	JN646000	JN647517
Bufo spinosus	BB154	Tunisia	Feija N. P. (loc. 1)	36°29′11.60″N	8°18′28.50″E	75	JN647202	JN647443				
Bufo spinosus	BB155	Tunisia	Feija N. P. (loc. 3)	36°29′51.10″N	8°18′19.20″E	76	JN647203	JN647444				
Bufo verrucosissimus circassicus	BB083	Russia	Krasnodar territory, Gelenjik district, Aderbiyevka	44°36′4.50″N	38°7′15.50″E	40	JN647233	JN647469	JN646956			
Bufo verrucosissimus circassicus	BB089	Russia	Krasnodar territory, Gelenjik, environs of Vozrozhdeniye, Zhene gorge	44°32′48.00″N	38°14′35.00″E	32	JN647236	JN647472				
Bufo verrucosissimus circassicus	BB090	Russia	Krasnodar territory, Gelenjik, Dzhankot environs	44°28′1.30″N	38°9′0.90″E	32	JN647237	JN647473				
Bufo verrucosissimus tertyschnikovi	BB058	Russia	Stavropol territory, Shpakovskiy district, Strizhament mt., environs	44°38′44.20″N	41°32′36.30″E	32	JN647226	JN647462	JN646959	JN646912	JN647008	JN647520
Bufo verrucosissimus tertyschnikovi	BB085	Russia	Stavropol territory, Shpakovskiy district, Novoyekaterinovskaya environs	44°45′58.50″N	42°2′4.50″E	32	JN647234	JN647470				
Bufo verrucosissimus turowi	BB057	Russia	Krasnodar territory, Caucasian Nature Reserve, environs of Chernorechye	43°55′59.40″N	40°39′45.30″E	32	JN647225	JN647461	JN646958	JN646911	JN647010	JN647519
Bufo verrucosissimus turowi	BB061	Russia	Krasnodar territory, Caucasian Nature Reserve, environs of Chernorechye	43°55′59.40″N	40°39′45.30″E	32	JN647229	JN647465				
Bufo verrucosissimus verrucosissimus	BB059	Georgia	Abkhazia, Bzypi gorge, Malaya Ritza lake	43°28′34.30″N	40°28′21.40″E	32	JN647227	JN647463		JN646914		JN647521
Bufo verrucosissimus verrucosissimus	BB060	Georgia	Adjaria, Charnali gorge, env. of Charnali	41°31′52.30″N	41°37′27.40″E	33	JN647228	JN647464	JN646960			JN647522
Bufo verrucosissimus verrucosissimus	BB063	Georgia	Borjomi valley, Bakuriani, Jagoras-Veli	41°43′30.20″N	43°31′8.20″E	33	JN647230	JN647466				
Bufo verrucosissimus verrucosissimus	BB064	Georgia	Borjomi valley, Akhaldaba river	41°52′56.50″N	43°21′30.50″E	35	JN647231	JN647467	JN646957	JN646910	JN647006	JN647523
Bufo verrucosissimus verrucosissimus	BB088	Russia	Krasnodar territory, Sochi district, Agura environs	43°46′20.50″N	39°37′22.70″E	43	JN647235	JN647471	JN646961	JN646915	JN647009	JN647524
Bufo verrucosissimus verrucosissimus	BB073	Turkey	Karagol	41°18′25.60″N	42°28′56.00″E	33	JN647232	JN647468	JN646962	JN646913	JN647007	JN647525
Outgroups												
Bufo bankorensis	BB098	China	Taiwan, Taipei environs, Fu Yang Shan N.P.	25°01′14.50″N	121°33′36.50″E	49	JN653290	JN653295	JN653310	JN653316	JN653301	JN653321
Bufo bankorensis	BB099	China	Taiwan, Taipei environs, Fu Yang Shan N.P.	25°01′14.50″N	121°33′36.50″E	50	JN653291	JN653296	JN653311		JN653302	JN653322
Bufo gargarizans gargarizans	BB096	China	Jilin province, SongJiangHe river, 50 km W from BaiTouShan (PekTuSan) volcano	42°9′3.50″N	127°30′44.50″E	47	JN647245	JN647481	JN653309			JN653319
Bufo gargarizans gargarizans	BB095	Russia	Jewish autonomous region, Bastak Nature Reserve, sq. 140	47°59′55.60″N	132°4′36.50″E	46	JN647244	JN647480	JN653308	JN653315	JN653300	JN653318
Bufo gargarizans gargarizans	BB097	Russia	Primorskiy (Maritime) territory, Partizansk district, Tigrovoy environs	43°9′17.30″N	132°53′0.30″E	48	JN647246	JN647482				
Bufo gargarizans sachalinensis	BB094	Russia	Sakhalin province, Sakhalin island, Tymovskiy district, Tym river, environs of Tymovskoye settlement	50°52′32.70″N	142°37′30.70″E	46	JN647243	JN647479				
Bufo japonicus formosus	BB101	Japan	Tokyo prefecture, Tokyo city, Sendagi	35°43′15.40″N	139°45′37.50″E	52	JN653293	JN653298	JN653306	JN653313	JN653304	JN653320
Bufo japonicus formosus	BB102	Japan	Aomori prefecture, Hirosaki city environs, Hirakawa	40°34′41.50″N	140°34′43.50″E	53	JN653294	JN653299	JN653307	JN653314		
Bufo torrenticola	BB100	Japan	Nara prefecture, Tenkawa environs	34°14′16.50″N	135°51′4.50″E	51	JN653292	JN653297	JN653305	JN653312	JN653303	JN653317

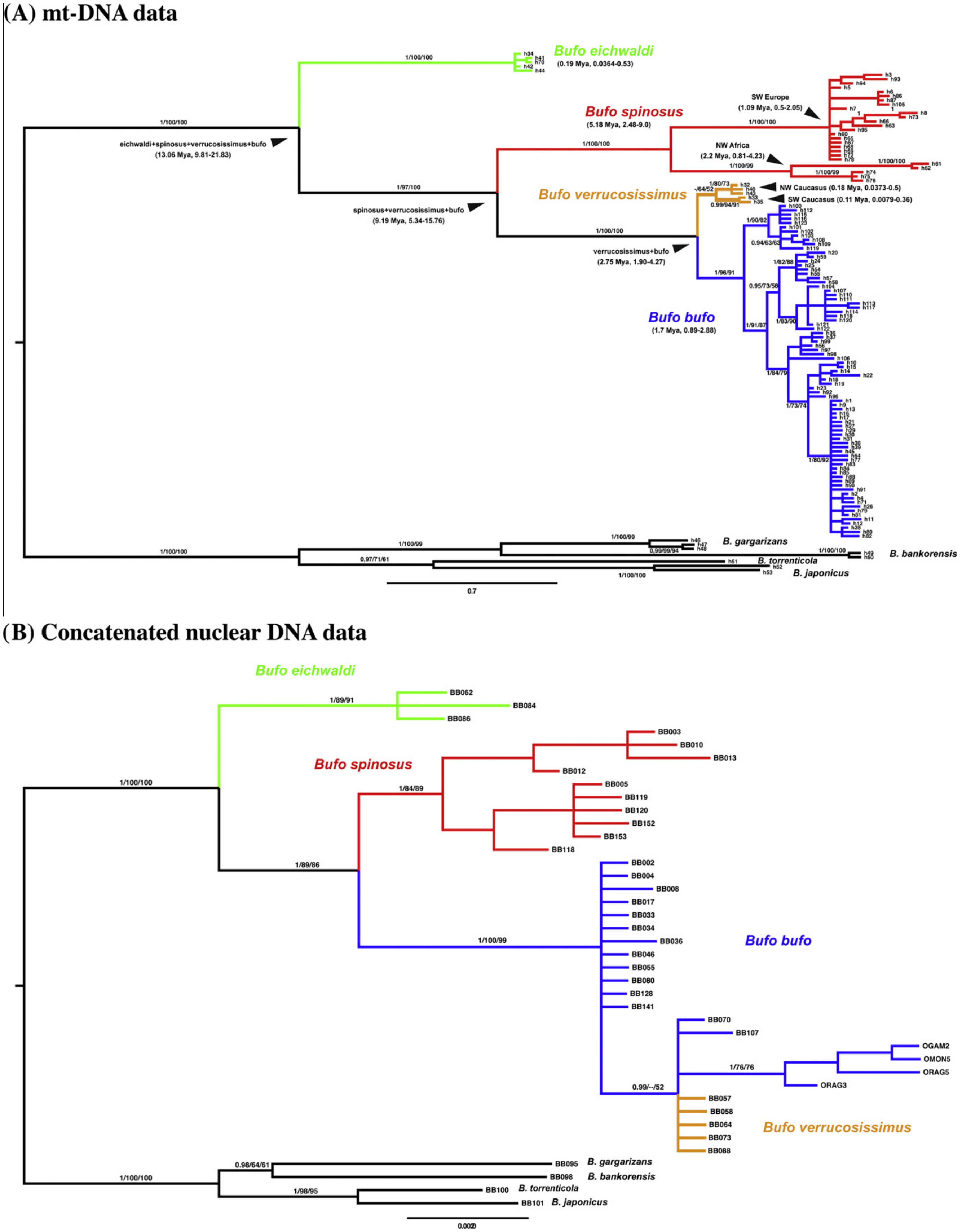
(A) mt-DNA data

(B) Concatenated nuclear DNA data

Fig. 2. Bayesian consensus phylograms based on mtDNA data (A) and the concatenated nuclear dataset (B). Support values in relevant branches are Bayesian posterior probabilities (only those >0.9 are shown), maximum likelihood (ML) and maximum parsimony (MP) bootstrap values, respectively. Estimated times to most recent common ancestor (TMRCA) for selected clades are shown in parentheses (median, 95% highest posterior density interval).

Table 2
Primer sequences used in this study.

Primer name	Sequence	Reference
16S-ar	CGC CTG TTT ATC AAA AAC AT	Palumbi et al. (1991)
16S-br	CCG GTC TGA ACT CAG ATC ACG T	Palumbi et al. (1991)
Cyt Bufo F	ATC TAC CTT CAC ATC GGA CGA G	This study
Cyt Bufo R	AGT TTR TTT TCT GTG AGT CC	This study
POMC_DRV_F1	ATA TGT CAT GAS CCA YTT YCG CTG GAA	Vieites et al. (2007)
POMC_DRV_R1	GGC RTT YTT GAA WAG AGT CAT TAG WGG	Vieites et al. (2007)
BUFO_CXCR4F	TTC TGG TCT GTG GAY GCY GCC ATT	This study
BUFO_CXCR4_R	TTG AGG CAG CAG TGG AAG AAG GCC	This study
BDNF_F1	ACC ATC CTT TTC CTK ACT ATG	This study
BDNF_R1	CTA TCT TCC CCT TTT AAT GGT	This study
RPL3buF1	AGG TGG CAG TGT CTG GAG TAT T	This study
RPL3buR1	GTC ACC TTA CTA CAG CTT GTT CTC A	This study

Table 3
Estimates of evolutionary divergence over sequence pairs between species as estimated by MEGA5. Mean values of *p*-uncorrected genetic distances and the corresponding standard errors are shown.

Species 1	Species 2	Mean *p*-uncorrected (%)	Std. error (%)
B. bufo	*B. spinosus*	7.0	0.6
B. bufo	*B. verrucosissimus*	1.6	0.3
B. spinosus	*B. verrucosissimus*	6.3	0.6
B. bufo	*B. eichwaldi*	7.3	0.7
B. spinosus	*B. eichwaldi*	7.7	0.7
B. verrucosissimus	*B. eichwaldi*	6.9	0.7

and species trees based on the multispecies coalescent (Figs. 2 and 3) strongly support our phylogenetic hypothesis.

The inferred species tree and time estimates derived from coalescent-based analyses of mtDNA data can be used to reconstruct the evolutionary history of the *B. bufo* species group (*B. bufo sensu lato* plus *B. eichwaldi* and *B. verrucosissimus*). In doing so, two facts must be kept in mind. First, TMRCA estimates refer to coalescence times in currently observed haplotype variants, and thus necessarily predate population divergence times. Although the magnitude of this difference between coalescence times and population divergence is hard to calculate (Rosenberg and Feldman, 2002), our estimates can still be informative about the relative timing of splitting events. Second, our TMRCA estimates are dependent on our choice of nodes for fossil calibration; in this respect the decision to use Miocene fossils to calibrate the minimum time for the deepest divergence between the four species seems the most appropriate with the data at hand (i.e., in the absence of diagnostic osteological characters distinguishing species). The scenarios derived from our analyses suggest a long evolutionary history of the *B. bufo* species group in western Europe, which is consistent with the fossil record, that includes abundant Pliocene sites in central Europe (Germany, Romania, Poland, Hungary, Slovakia) and the Apennine and Iberian peninsulas, and Pleistocene fossils in North Africa (Morocco) (see Martín and Sanchiz, 2011) (Fig. 4).

According to our median TMRCA estimates, and taking into account the uncertainty reflected in their corresponding HPDIs, the initial split between *B. eichwaldi* and the other species would have taken place in the Miocene, between about 13 and 9 Mya [which are the estimated TMRCAs of (*eichwaldi* + *spinosus* + *bufo* + *verrucosissimus*) and the latter three species, respectively], considerably older that previously estimated based on allozyme data (Litvinchuk et al., 2008) (Fig. 4A). This biogeographic pattern (Europe-Caucasus split) is recurrent across groups, with other amphibian examples including Parsley frogs (genus *Pelodytes*), which have species in the Iberian Peninsula, France and northwestern Italy (*P. punctatus* and *P. ibericus*) and in the Caucasus (*P. caucasicus*) (García-París et al., 2003; Veith et al., 2006); and salamanders (the Iberian *Chioglossa lusitanica* and *Mertensiella caucasica* in the Caucasus) (Veith et al., 1998; Zhang et al., 2008). The uplift of the Armenian Plateau and the opening of the Mid-Aegean Trench during the Miocene, which have been invoked to explain similar patterns in other groups (see Wielstra et al. (2010) and references cited therein), might also be associated with this split in the *B. bufo* species group. Our data show contrasting patterns of genetic diversity in the current descendants of these two ancient lineages. *Bufo eichwaldi* presents low intraspecific genetic diversity, although perhaps denser sampling across its range (particularly towards the Iranian end of the distribution) might reveal the existence of additional sublineages. On the other hand, species with restricted ranges are especially sensitive to major climate fluctuations, and Pleistocene glaciations may have had a major impact on genetic diversity in *B. eichwaldi*, as has been the case for other species that were marginally distributed in refugium areas during that period (Recuero and García-París, 2011). This isolation might have also prevented secondary contact and introgression with other species in the group. At present at least 250 km of unsuitable woodless lowland area separates populations of *B. eichwaldi* from the nearest populations of *B. verrucosissimus* (a few records of *B. bufo* species group from central Azerbaijan require confirmation). There is no evidence of introgression between both species based on our nDNA analyses. Litvinchuk et al. (2008) reported seven diagnostic allozyme loci out of 24 analyzed between the two species. The Hyrcanian broad-leaved subtropical forests of Talysh and Elburz mountains are known as a relic of the Tertiary vegetation, which formerly had a much broader distribution in NW Eurasia (see Tuniyev (1999) and references cited therein). This area harbors a number of endemic amphibian and reptile species and lineages (e.g. *Paradactylodon persicus*, *Rana pseudodalmatina*, *Darevskia chlorogaster*, *D. defilippii*, *Zamenis persicus*, *Gloydius* (*halys*) *caucasicus*). Our phylogenetic scenario for the *B. bufo* species group provides further evidence that the Hyrcanian refugium played an important role in the formation of modern herpetological diversity of the Caucasus, Anatolia and Europe.

After the initial split, the ancestor of western European species gave rise to a much more genetically and morphologically diverse lineage, where three extant species can be readily identified. Most variation in these species is concentrated in the three major Pleistocene refugia in Western Europe: the Iberian, Apennine and Balkan peninsulas, as typically found in other widely distributed organisms in the western Palearctic (e.g., Zeisset and Beebee, 2008). This pattern can be explained by the isolation and persistence through climatic cycles of old (Miocene and Pliocene) toad lineages, mainly in North Africa, the Caucasus and the Mediterranean peninsulas. The splitting of *B. spinosus* from the ancestor of *B. bufo* + *B. verrucosissimus* might be associated with the different phases of the uplift of the Pyrenees, which isolated the Iberian peninsula from the rest of western Europe during most of the Tertiary and ended about 5 million years ago (Plaziat, 1981; Oosterbroek and Arntzen, 1992) (Fig. 4B). Based on our TMRCA estimates, the split between north African and Iberian populations of *B. spinosus* probably took place at the end of the Messinian Salinity Crisis 5.3 Mya or slightly thereafter (see Hewitt (2011) and references cited therein) (Fig. 4C). Busack (1986) found three fixed allozyme differences between populations on both sides of the Strait of Gibraltar, with a genetic distance (D_{Nei}) of 0.16, which is consistent with this hypothesis, although more detailed assessments of North African populations, which are small and fragmented, are needed. Although no obvious pattern of genetic structure was found in Iberian populations of *B.*

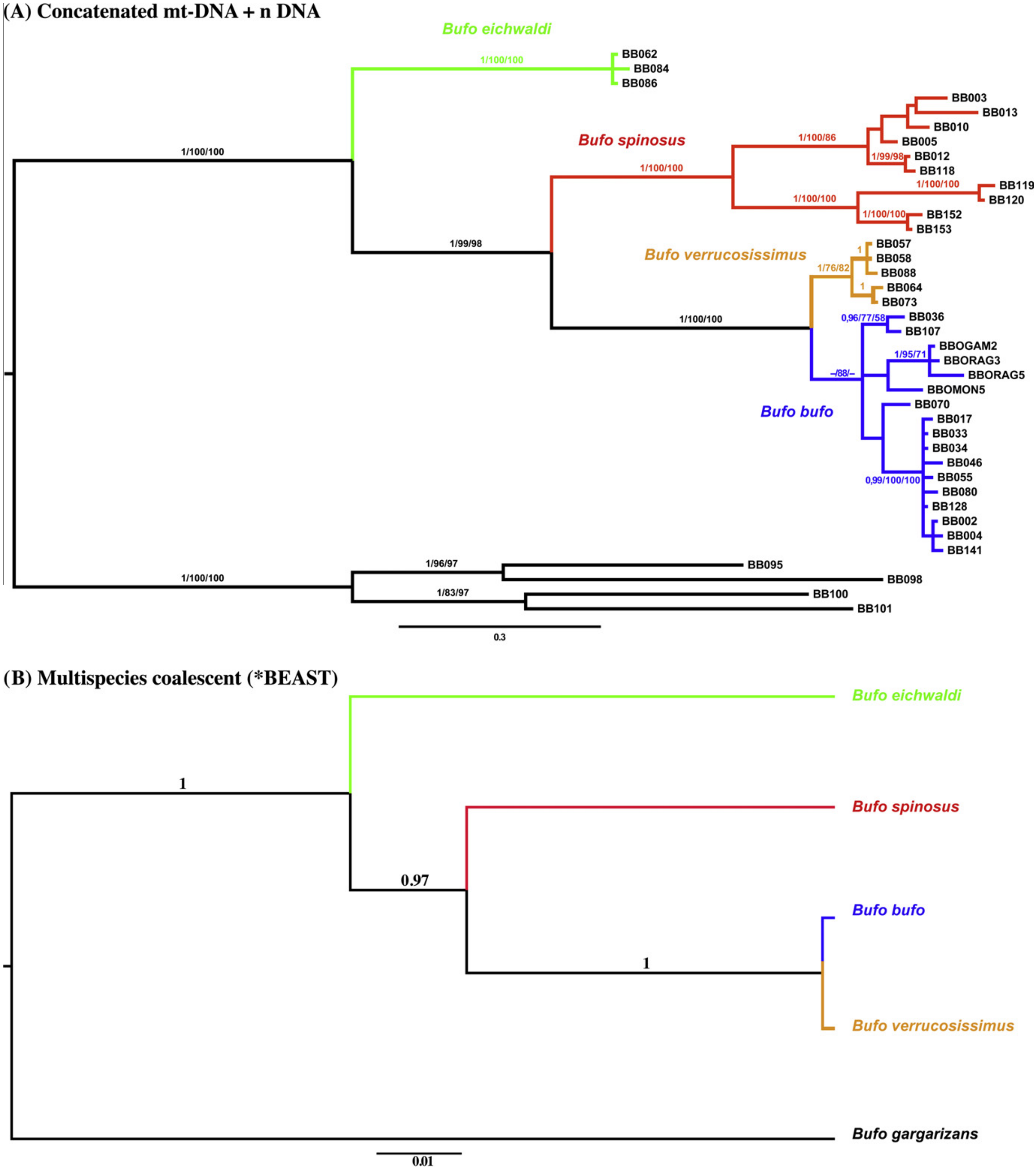

Fig. 3. Bayesian consensus phylogram based on concatenated analysis of mitochondrial and nuclear DNA (A), and species tree based on the multispecies coalescent implemented in *BEAST (B). Support values in relevant branches are Bayesian posterior probabilities (only those >0.9 are shown), and, where applicable (Fig. 3A), maximum likelihood (ML) and maximum parsimony (MP) bootstrap values, respectively.

bufo, as reported by Martínez-Solano and González (2008), populations in southern Iberia and the Sistema Central Mountains in central Spain (including Gredos, from where *B. b. gredosicola* was described) do seem to harbor considerable genetic diversity. Future studies should use more variable markers from the nuclear genome and denser population sampling in order to further unravel the evolutionary history of *B. spinosus* across its range.

Finally, *B. bufo* and *B. verrucosissimus* appear to have split recently, in the Pleistocene (Fig. 4D). Mitochondrial DNA distances are low with respect to typical values found in other amphibian species pairs (but see also *Triturus marmoratus*/*Triturus* pygmaeus or *Pelodytes punctatus*/*Pelodytes ibericus*, García-París et al., 2001, 2003; Veith et al., 2006; Wielstra and Arntzen, 2011), but this may reflect recent divergence (as indicated by incomplete lineage

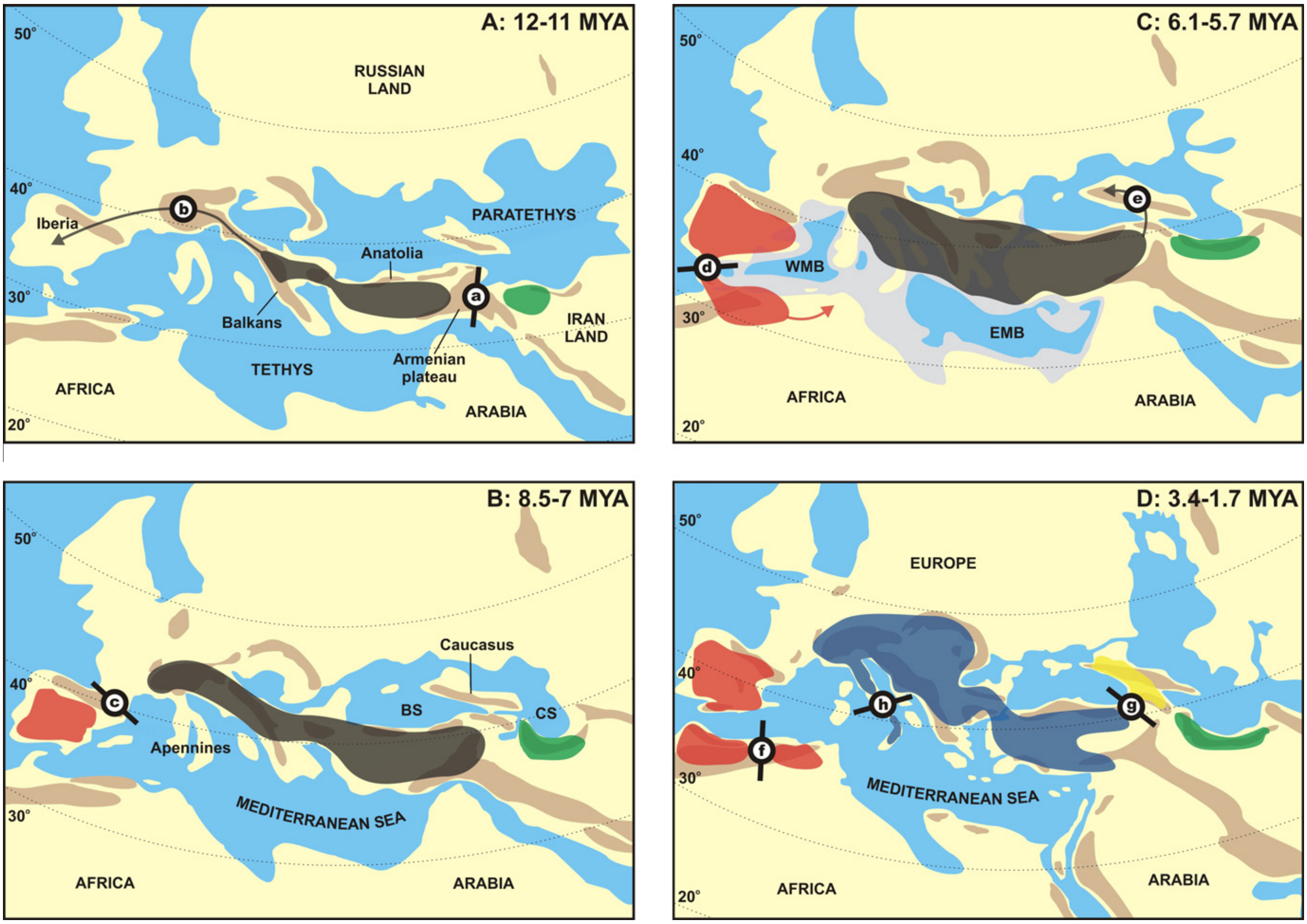

Fig. 4. Paleogeographic reconstructions and major cladogenetic events in *Bufo bufo* (modified from Popov et al. (2004) and Wielstra et al. (2010)). Events are marked with letters (a–g); range colors as in Figs. 1–3; inferred ancestor ranges in black. (A) Late–Middle Miocene: the movement of African and Arabian plates towards the European archipelago leads to extensive orogenesis (shaded light brown) in the Near and Middle East and the uplift of the Armenian Plateau; this isolates the ancestor of *B. eichwaldi* from the common ancestor of other clades inhabiting the Balkan–Anatolian landmass (**a**; 13–9 Mya); orogenetic processes in the Dinarian and Alp regions create a land bridge which allows the dispersal of the ancestor of *B. bufo*, *B. verrucosissimus* and *B. spinosus* to the west (**b**). (B) Mid–Late Miocene: extensive orogenesis and formation of the Neo-Pyrenees isolates the ancestor of *B. spinosus* in the Iberian peninsula from the ancestor of *B. bufo* and *B. verrucosissimus* (**c**; 9.19 Mya). (C) Late Miocene: the Messinian Salinity Crisis (MSC) led to dramatic sea level drop in the Mediterranean Basin (exposed parts of sea bottom shaded in light gray), including a land bridge between Iberia and N Africa, allowing *B. spinosus* to disperse southwards; subsequent rise of sea level after the MSC isolates N African populations (**d**; 5.18 Mya); Caucasia gradually becomes connected with Anatolian land, allowing the ancestor of *B. bufo* and *B. verrucosissimus* to colonize the area (**e**). D) Middle–Late Pliocene: the marine connection between the Atlantic ocean, Mediterranean and Ponto-Caspian basins is re-established, Caucasia gradually becomes an isthmus between the Black and Caspian seas; intensification of orogenesis, periodical drops in global sea level and/or climatic oscillations during the Pleistocene cause the split between *B. verrucosissimus* in Caucasia and *B. bufo* (**g**; 2.75 Mya) and intraspecific differentiation: split within N African clade of *B. spinosus* (**f**; 2.20 Mya) and separation of S Italian clade of *B. bufo* (**h**; 1.70 Mya). *Abbreviations*: **WMB** – West Mediterranean Basin; **EMB** – East Mediterranean Basin; **BS** – Black Sea; **CS** – Caspian Sea.

sorting in nuclear markers), perhaps with some gene flow (some of the patterns observed in the nuclear DNA topologies are consistent with this interpretation, with shared alleles between *verrucosissimus* and Anatolian *B. bufo* in some markers, see also the combined nDNA tree in Fig. 2B). In spite of these patterns, previous studies have documented the distinctiveness of *B. verrucosissimus* based on morphological, ecological, and biochemical characters (Birschtein and Mazin, 1982; Orlova and Tuniyev, 1989; Kuzmin, 1999; Pisanets et al., 2009), and there is some evidence that, whereas both species can interbreed in laboratory conditions, hybrid survival may not exceed the second generation (see Pisanets, 2001, 2002; Pisanets et al., 2009).

During the Pleistocene, major haplogroups within *B. spinosus* in North Africa and the Iberian Peninsula originated (Fig. 4D), and the same is true for well-resolved subclades within *B. bufo* and *B. verrucosissimus*. Within the latter up to four morphological subspecies were recognized, with *B. v. verrucosissimus* occupying the major part of the species distribution in Georgia and along the southern slopes of the Great Caucasus, and *B. v. turowi*, *B. v. circassicus*, and *B. v. tertyschnikovi* occupying mountain areas in the northwest periphery of the species range (Orlova and Tuniyev, 1989; Kidov, 2009). Despite significant interspecific variation of certain morphological characters, their validity has been doubted recently (Litvinchuk et al., 2008; Pisanets et al., 2009). The subclades of *B. verrucosissimus* we recovered do not correspond to current subspecific designations, rather they correspond to the two major allopatric population groups from southern and northern parts of the species range and, pending more detailed morphological and ecological studies, may be regarded as independent management units in conservation planning. Our results also provide the first genetic evidence for the presence of *B. verrucosissimus* in Turkey (Karagol), which was not yet confirmed (Eiselt, 1965; Baran and Atatur, 1998; Kutrup et al., 2006), and also clearly indicate that most of Anatolia is inhabited by *B. bufo* (*s. str.*), in contrast with Litvinchuk et al.'s (2008) assumption that the name *B. v. verrucosissimus* should be applied to all Anatolian populations.

In *B. bufo* there is a sharp contrast between the high genetic diversity observed in the south (especially in the Apennine and Balkan peninsulas) and the genetic homogeneity of populations in the north, with haplotype sharing in samples from central and northern Europe being fairly common. Brede and Beebee (2006) found remarkably little genetic differentiation in *B. bufo* populations across most of Europe based on microsatellite markers. Although they did not find a deep break between populations of *B. bufo* and *B. spinosus* in their study, samples from Iberia and south France showed deviations from Hardy–Weinberg equilibrium that could reflect the occurrence of null alleles in these populations and some of them were thus not included in interpopulation comparisons. In any case, their results also suggest a very rapid colonization potential for the species, since the areas that are now occupied by populations nested in the less genetically diverse clade within *B. bufo* were covered by glaciers and tundra until the end of the Last Glacial Maximum (Hewitt, 1999; CGMW–ANDRA, 1999). Based on our phylogenetic analyses, the source of this colonization could have been the Balkan Peninsula (Fig. 2) – in a pattern very similar to that observed in other amphibians, like *Lissotriton vulgaris* (see Babik et al., 2005) – or some neighboring area (see e.g. Hofman et al., 2007; Sotiropoulos et al., 2007; Canestrelli and Nascetti, 2008).

Our results also allow delineation of the ranges of *B. bufo* and *B. spinosus,* which has long been an issue in morphological, ecological, genetic and conservation studies (Daudin, 1803; Mertens and Wermuth, 1960; Hemmer and Böhme, 1976; Lüscher et al., 2001; IUCN, 2009). The type locality of *B. spinosus* is "aux environs de Brives et de Bordeaux", in southern France (Frost, 2011), well within the range of our *spinosus* clade. According to our data, therefore, *B. spinosus* includes all populations in the Maghreb, the Iberian Peninsula and parts of France. The genetic distinctiveness in all markers examined with respect to *B. bufo* support its recognition at the species level, although a reappraisal of morphological and ecological variation within and between species in the group, based on current species limits, is still desired. Preliminary location of contact zones with *B. bufo* based on spatial patterns of mtDNA haplotype sharing points to: (1) the Maritime Alps between SE France and NW Italy (sample codes: OBYX, see Table 1 and Fig. 1), which is a well-known suture zone (*sensu* Swenson and Howard, 2005) for other species (see for example, Kropf et al., 2002) and (2) northern France, where there is a striking parallelism with the contact zone between the newts *Triturus cristatus* and *T. marmoratus* (Arntzen and Wallis, 1991; Arntzen et al., 2009). These areas are worth of further fine-scale studies on the formation and maintenance of reproductive barriers between species. On the other hand, *B. bufo* would be distributed in northern France and the rest of Western Europe to Siberia, including the Apennine and Balkan peninsulas and most of Anatolia. The eastern limits and the potential existence of contact zones with *B. verrucosissimus* are still unclear, although our study will also help identify relevant areas for further study.

Our study is the first to analyze a geographically comprehensive sampling including all described species and subspecies in the *B. bufo* species group. The combined use of molecular markers from the nuclear and mitochondrial genomes and the adoption of a variety of analytical approaches including species tree estimation produced a fully resolved topology which will set the basis for the clarification of the taxonomy, systematics, and evolutionary history of the group and will serve as a foundation for further studies on the process of species formation.

Acknowledgments

Special thanks to M. Tuschek and the late Á. Major for technical support. D. Buckley provided helpful comments on the manuscript. L. J. Barbadillo, B. Baudin, J. Ben Hassine, T. Burke, Y-H. Chang, M. Denoël, V. V. Dernakov, E. Dunayev, J. Dinov, A. Fouquet, M. García-París, P. Geissler, A. Grande, C. Grande, J. Gutiérrez, G. Herczeg, K. Iizuka, R. Jehle, D. Jelić, A. Kotán, M. Kuro-o, P. Lymberakis, K. A. Matushkina, P. Mikuliček, T. Németh, S. Nouira, A. Ogrodowczyk, L. Pongó, I. A. Serbinova, T. Shibata, N. Smiljković, F. Spallone, F. Speranza, J. van Alphen, A. Vassilieva, G. Wallis, B. Wielstra, O. Zinenko, and A. Zuiderwijk provided samples and/or support during field trips, and I. Rey and B. Álvarez (Colección de Tejidos y ADN, MNCN) provided samples under their care. IMS is a "Ramón y Cajal" postdoctoral fellow supported by the Spanish Ministerio de Ciencia e Innovación and the Universidad de Castilla la Mancha. The Synthesis Project (http://www.synthesys.info/) of the European Union partially supported this study (Ref.: HU-TAF-181). Partial funds were also provided by the Spanish Ministerio de Ciencia e Innovación (Ref.: CGL2008-04271-C02-01/ BOS) and Junta de Comunidades de Castilla la Mancha (Ref.: PPII10-0097-4200) to IMS, Hungarian Scientific Research Fund (OTKA K77841) to JV and Ministry of Education and Science of Republic of Serbia (Grant No. 173025) to JCI.

Appendix A. Supplementary data

Supplementary data associated with this article can be found, in the online version, at doi:10.1016/j.ympev.2011.09.008.

References

Aldenhoven, J., Miller, M., Corneli, P., Shapiro, M., 2010. Phylogeography of ninespine sticklebacks (*Pungitius pungitius*) in North America: glacial refugia and the origins of adaptive traits. Mol. Ecol. 19, 4061–4076.

Arntzen, J.W., Wallis, G.P., 1991. Restricted gene flow in a moving hybrid zone of the newts *Triturus cristatus* and *T. marmoratus* in Western France. Evolution 45, 805–826.

Arntzen, J., Jehle, R., Bardakci, F., Burke, T., Wallis, G., 2009. Asymmetric viability of reciprocal-cross hybrids between crested and marbled newts (*Triturus cristatus* and *T. marmoratus*). Evolution 63, 1191–1202.

Arora, N., Nater, A., Van Schaik, C., Willems, E.P., Van Noordwijk, M., Goossens, B., Morf, N., Bastian, M., Knott, C., Morrogh-Bernard, H., Kuze, N., Kanamori, T., Pamungkas, J., Perwitasari-Farajallah, D., Verschoor, E., Warren, K., Krützen, M., 2010. Effects of Pleistocene glaciations and rivers on the population structure of Bornean orangutans (*Pongo pygmaeus*). Proc. Natl. Acad. Sci. USA 107, 21376–21381.

Babik, W., Branicki, W., Crnobrnja-Isailovic, J., Cogălniceanu, D., Sas, I., Olgun, K., Poyarkov, N.A., García-París, M., Arntzen, J.W., 2005. Phylogeography of two European newt species. Discordance between mtDNA and morphology. Mol. Ecol. 14, 2475–2491.

Baran, I., Atatur, M.K., 1998. Turkish herpetofauna (Amphibians and Reptiles). Republic of Turkey Ministry of Environment, Ankara, 214p.

Birschtein, V.J., Mazin, A.L., 1982. Chromosomal polymorphism of *Bufo bufo*: karyotype and C-banding pattern of *B. b. verrucosissima*. Genetica 59, 93–98.

Blackburn, D.C., Bickford, D.P., Diesmos, A.C., Iskandar, D.T., Brown, R., 2010. An ancient origin for the enigmatic flat-headed frogs (Bombinatoridae: *Barbourula*) from the islands of southeast Asia. PLoS ONE 5, e12090.

Brede, E.G., Beebee, T.J.C., 2006. Consistently different levels of genetic variation across the European ranges of two anurans, *Bufo bufo* and *Rana temporaria*. Herpetol. J. 16, 265–271.

Bruen, T.C., Philippe, H., Bryant, D., 2006. A simple and robust statistical test for detecting the presence of recombination. Genetics 172, 2665–2681.

Busack, S.D., 1986. Biogeographic analysis of the herpetofauna separated by the formation of the Strait of Gibraltar. Natl. Geogr. Res. 2, 17–36.

Canestrelli, D., Nascetti, G., 2008. Phylogeography of the pool frog *Rana* (*Pelophylax*) *lessonae* in the Italian peninsula and Sicily: multiple refugia, glacial expansions and nuclear–mitochondrial discordance. J. Biogeogr. 35, 1923–1936.

CGMW–ANDRA, 1999. Maps of the World Environments During the Last Two Climatic Extremes: 1. The Last Glacial Maximum (ca 18,000 + 2000 yrs BP), 2. The Holocene Optimum (ca 8000 + 1000 yrs BP) (1:25,000,000 scale). Commission for the Geological Map of the World (CGMW), Paris and the Agence Nationale pour la Gestion des Déchets Radioactifs (ANDRA), Chatenay-Malabry, France.

Chkhikvadze, V.M., 1984. Review of fossil urodeles and anurans of the USSR. Izv. AN GrSSR Ser. Biol. 10, 5–13.

Chung, Y., Ané, C., 2011. Comparing two Bayesian methods for gene tree/species tree reconstruction: simulations with incomplete lineage sorting and horizontal gene transfer. Syst. Biol. 60, 261–275.

Daudin, F.M., 1803. Histoire Naturelle, génerale et particulière des Reptiles. T. 8, Imprimerie de F. Dufart, Paris.

De Lange, L., 1973. A contribution to the intraspecific systematics of *Bufo bufo* (Linnaeus, 1758) (Amphibia). Beaufortia 21, 99–116.

Drummond, A.J., Rambaut, A., 2007. BEAST: Bayesian evolutionary analysis by sampling trees. BMC Evol. Biol. 7, 214.

Dubois, A., Bour, R., 2010. The nomenclatural status of the nomina of amphibians and reptiles created by Garsault (1764), with a parsimonious solution to an old nomenclatural problem regarding the genus *Bufo* (Amphibia, Anura), comments on the taxonomy of this genus, and comments on some nomina created by Laurenti (1768). Zootaxa 2447, 1–52.

Edwards, S.V., 2009. Is a new and general theory of molecular systematics emerging? Evolution 63, 1–19.

Eiselt, J., 1965. Einige Amphibien und Reptilien aus der Nordoslichen Turkei, gesammelt von Hern H. Steiner. Annu. Natur Histor. Mus. Wien 67, 387–389.

Frost, D., 2011. Amphibian Species of the World: An Online Reference. Version 5.5 (31 January, 2011). American Museum of Natural History, New York, USA. <http://research.amnh.org/vz/herpetology/amphibia/>.

Frost, D., Grant, T., Faivovich, J., Bain, R., Haas, A., Haddad, C.F.B., De Sa, R.O., Channing, A., Wilkinson, M., Donnellan, S.C., Raxworthy, C., Campbell, J., Blotto, B., Moler, P., Drewes, R., Nussbaum, R., Lynch, J., Green, D., Wheeler, W., 2006. The amphibian tree of life. Bull. Am. Mus. Nat. Hist. 297, 1–370.

Fu, Y.-X., Li, W.-H., 1993. Statistical tests of neutrality of mutations. Genetics 133, 693–709.

Fu, J., Weadick, C., Zeng, X., Wang, Y., Liu, Z., Zheng, Y., Li, C., Hu, Y., 2005. Phylogeographic analysis of the *Bufo gargarizans* species complex: a revisit. Mol. Phylogenet. Evol. 37, 202–213.

García-París, M., Arano, B., Herrero, P., 2001. Molecular characterization of the contact zone between *Triturus pygmaeus* and *T. marmoratus* (Caudata: Salamandridae) in Central Spain and their taxonomic assessment. Rev. Esp. Herp. 15, 115–126.

García-París, M., Buchholz, D., Parra-Olea, G., 2003. Phylogenetic relationships of Pelobatoidea re-examined using mtDNA. Mol. Phylogenet. Evol. 28, 12–23.

García-París, M., Montori, A., Herrero, P., 2004. Amphibia, Lissamphibia. In: Ramos, M.A. et al. (Eds.), Fauna Iberica, vol. 24. Museo Nacional de Ciencias Naturales, CSIC, Madrid, Spain, pp. 1-640.

Guindon, S., Gascuel, O., 2003. A simple, fast and accurate method to estimate large phylogenies by maximum-likelihood. Syst. Biol. 52, 696–704.

Gumilevskij, B.A., 1936. Notes on some Batrachia of the Eastern Palearctic Fauna. Trudy Zoologicheskogo Instituta. USSR Acad. Sci. Leningrad 4, 167–171.

Gvozdík, V., Moravec, J., Klütsch, C., Kotlík, P., 2010. Phylogeography of the Middle Eastern tree frogs (*Hyla*, Hylidae, Amphibia) as inferred from nuclear and mitochondrial DNA variation, with a description of a new species. Mol. Phylogenet. Evol. 55, 1146–1166.

Heled, J., Drummond, A.J., 2010. Bayesian inference of species trees from multilocus data. Mol. Biol. Evol. 27, 570–580.

Hemmer, H., Böhme, W., 1976. Zwischenbericht über die innerartliche Variabilität der Erdkröte (*Bufo bufo* L) (Amphibia: Salentia: Bufonidae). Salamandra 12, 194–201.

Hewitt, G.M., 1999. Post-glacial re-colonization of European biota. Biol. J. Linn. Soc. 68, 87–112.

Hewitt, G.M., 2011. Mediterranean Peninsulas—the evolution of hotspots. In: Zachos, F.E., Habel, J.C. (Eds.), Biodiversity Hotspots. Springer, Amsterdam, pp. 123–148.

Hofman, S., Spolsky, C., Uzzell, T., Cogălniceanu, D., Babik, W., Szymura, J., 2007. Phylogeography of the fire-bellied toads *Bombina*: independent Pleistocene histories inferred from mitochondrial genomes. Mol. Ecol. 16, 2301–2316.

Huelsenbeck, J.P., Ronquist, F., 2001. MrBayes: Bayesian inference of phylogeny. Bioinformatics 17, 754–755.

Huson, D.H., Bryant, D., 2006. Application of phylogenetic networks in evolutionary studies. Mol. Biol. Evol. 23, 254–267.

Igawa, T., Kurabayashi, A., Nishioka, M., Sumida, M., 2006. Molecular phylogenetic relationship of toads distributed in the Far East and Europe inferred from the nucleotide sequences of mitochondrial DNA genes. Mol. Phylogenet. Evol. 38, 250–260.

Inger, R.F., 1972. *Bufo* of Eurasia. In: Blair, W.F. (Ed.), Evolution in the Genus *Bufo*. Univ. Texas Press, Austin–London, pp. 102–118.

IUCN Red List of Threatened Species. Version 2009.1. <www.iucnredlist.org> (downloaded 16.06.11).

Kidov, A.A., 2009. Caucasus common toad *Bufo verrucosissimus* (Pallas, [1814]) (Amphibia, Anura, Bufonidae) in Western and Central pre-Caucasia: notes on distribution and taxonomy. Sci. Res. Zool. Parks 25, 170–179.

Kropf, M., Kadereit, J.W., Comes, H.P., 2002. Late Quaternary distributional stasis in the submediterranean mountain plant *Anthyllis montana* L. (Fabaceae) inferred from ITS sequences and amplified fragment length polymorphism markers. Mol. Ecol. 11, 447–463.

Kubatko, L.S., Carstens, B.C., Knowles, L.L., 2009. STEM: species tree estimation using maximum likelihood for gene trees under coalescence. Bioinformatics 25, 971–973.

Kutrup, B., Yilmaz, N., Canakci, S., Belduz, A., Doglio, S., 2006. Intraspecific variation of *Bufo bufo*, based on 16S Ribosomal RNA sequences. Amphibia–Reptilia 27, 268–273.

Kuzmin, S.L., 1999. The Amphibians of the Former Soviet Union. KMK, Moscow.

Librado, P., Rozas, J., 2009. DnaSP v5: a software for comprehensive analysis of DNA polymorphism data. Bioinformatics 25, 1451–1452.

Litvinchuk, S., Borkin, L., Skorinov, D.V., Rosanov, J.M., 2008. A new species of common toads from the Talysh mountains, south-eastern Caucasus: genome size, allozyme, and morphological evidences. Russ. J. Herpetol. 15, 19–43.

Liu, W., Lathrop, A., Fu, J., Yang, D., Murphy, R., 2000. Phylogeny of East Asian bufonids inferred from mitochondrial DNA sequences (Anura: Amphibia). Mol. Phylogenet. Evol. 14, 423–435.

Liu, L., Pearl, D.K., Brumfield, R.T., Edwards, S.V., Knowles, L.L., 2008. Estimating species trees using multiple-allele DNA sequence data. Evolution 62, 2080–2091.

Lüscher, B., Grossenbacher, K., Scholl, A., 2001. Genetic differentiation of the common toad (*Bufo bufo*) in the Swiss Alps. Amphibia–Reptilia 22, 141–154.

Macey, J.R., Schulte, J.A., Larson, A., Fang, Z., Wang, Y., Tuniyev, B.S., Papenfuss, T.J., 1998. Phylogenetic relationships of toads in the *Bufo bufo* species group from the eastern escarpment of the Tibetan Plateau: a case of vicariance and dispersal. Mol. Phylogenet. Evol. 9, 80–87.

Martín, C., Sanchiz, B., 2011. Lisanfos KMS. Version 1.2. Museo Nacional de Ciencias Naturales, MNCN-CSIC. Madrid, Spain. <http://www.lisanfos.mncn.csic.es/>.

Martínez-Solano, I., González, E.G., 2008. Patterns of gene flow and source-sink dynamics in high altitude populations of the common toad *Bufo bufo* (Anura: Bufonidae). Biol. J. Linn. Soc. 95, 824–839.

Matsui, M., 1980. Karyology of the Eurasian toads of the *Bufo bufo* complex. Annotationes Zoologicae Japonenses/Nihon dbutsugaku ih. Tokyo 53, 56–68.

Matsui, M., 1984. Morphometric variation analyses and revision of the Japanese toads (genus *Bufo*, Bufonidae). Contrib. Biol. Lab., Kyoto Univ. 26, 209–428.

Matsui, M., 1986. Geographic variation in toads of the *Bufo bufo* complex from the Far East, with a description of a new subspecies. Copeia 1986, 561–579.

Mertens, R., Wermuth, H., 1960. Die Amphibien und Reptilien Europas (Dritte Liste, nach dem Stand vom 1. Januar 1960). Waldemar Kramer, Frankfurt am Main.

Nei, M., 1987. Molecular Evolutionary Genetics. Columbia University Press, New York, USA.

Oosterbroek, P., Arntzen, J.W., 1992. Area-cladograms of Circum-Mediterranean taxa in relation to Mediterranean palaeography. J. Biogeogr. 19, 3–20.

Orlova, V.F., Tuniyev, B.S., 1989. On the taxonomy of the Caucasian common toads belonging to the group *Bufo bufo verrucosissimus* (Pallas) (Amphibia, Anura, Bufonidae). Bull. Mosk. Obshch. Isp. Prirody Ser. Biol. 94, 13–24.

Palumbi, S., Martin, A., Romano, S., McMillan, W.O., Stice, L., Grabowski, G., 1991. The Simple Fool's Guide to PCR. Version 2. Department of Zoology and Kewalo Marine Laboratory. University of Hawaii, Hawaii, USA.

Pisanets, E.M., 2001. Taxonomic relationships of the common toads (*Bufo bufo* complex) and some theoretical and practical problems of systematics. Communication 1. Vestn. Zool. Kiev 35, 37–44.

Pisanets, E.M., 2002. Taxonomic relationships of the common toads (*Bufo bufo* complex) and some theoretical and practical problems of systematics. Communication 2. Vestn. Zool. Kiev 36, 61–68.

Pisanets, Y.M., Litvinchuk, S.N., Rosanov, Yu.M., Reminniy, V.Yu., Pasinkova, R.A., Suryadnaya, N.N., Matvyeyev, A.S., 2009. Common toads (Amphibia, Bufonidae, *Bufo bufo* complex) from the Ciscaucasia and North Caucasus: the new analysis of the problem. Sbornik Prats Zologichnogo Muzeyu (Kiev) 40, 87–129.

Plaziat, J.-C., 1981. Late Cretaceous to Late Eocene palaeogeographic evolution of southwest Europe. Palaeogeogr. Palaeoclimatol. Palaeoecol. 36, 263–320.

Popov, S.V., Ilyina, L.B., Paramonova, N.P., Goncharova, I.A., et al., 2004. Lithological–paleogeographic maps of Paratethys. Cour. Forsch.Inst. Senckenb. 250, 1–46.

Posada, D., 2008. JModelTest: phylogenetic model averaging. Mol. Biol. Evol. 25, 1253–1256.

Rambaut, A., Drummond, A.J., 2007. Tracer v1.4. <http://beast.bio.ed.ac.uk/Tracer>.

Ratnikov, Y.V., 2001. Osteology of Russian toads and frogs for paleontological researches. Acta Zool. Cracov. 44, 1–23.

Recuero, E., García-París, M., 2011. Evolutionary history of *Lissotriton helveticus*: multilocus assessment of ancestral vs. recent colonization of the Iberian Peninsula. Mol. Phylogenet. Evol. 60, 170–182.

Rosenberg, N.A., Feldman, M.W., 2002. The relationship between coalescence times and population divergence times. In: Slatkin, M., Veuille, M. (Eds.), Modern Developments in Theoretical Population Genetics. Oxford University Press, Oxford, pp. 130–164.

Salicini, I., Ibáñez, C., Juste, J., in press. Multilocus phylogeny and species delimitation within the Natterer's bat species complex in the Western Palearctic. Mol. Phylogenet. Evol.

Sanguila, M.B., Siler, C.D., Diesmos, A.C., Nuñeza, O., Brown, R., 2011. Phylogeography and conservation implications of geographic structure, genetic variation, and potential species boundaries in Philippine slender toads. Mol. Phylogenet. Evol. 61, 333–350.

Sinsch, U., Schneider, H., Tarkhnishvili, D., 2009. *Bufo bufo* Superspezies – Erdkröten-Artenkreis. In: Grossenbacher, K. (Ed.), Handbuch der Reptilien und Amphibien Europas, vol. 5. Aula Verlag, Wiesbaden, pp. 187–337.

Sotiropoulos, K., Eleftherakos, K., Džukić, G., Kalezić, M., Legakis, A., Polymeni, R., 2007. Phylogeny and biogeography of the alpine newt *Mesotriton alpestris* (Salamandridae, Caudata), inferred from mtDNA sequences. Mol. Phylogenet. Evol. 45, 211–226.

Stöck, M., Moritz, C., Hickerson, M., Frynta, D., Dujsebayeva, T., Eremchenko, V., Macey, J.R., Papenfuss, T.J., Wake, D.B., 2006. Evolution of mitochondrial relationships and biogeography of Palearctic green toads (*Bufo viridis* subgroup) with insights in their genomic plasticity. Mol. Phylogenet. Evol. 41, 663–689.

Stöck, M., Sicilia, A., Belfiore, N.M., Buckley, D., Lo Brutto, S., Lo Valvo, M., Arculeo, M., 2008. Post-Messinian evolutionary relationships across the Sicilian channel: Mitochondrial and nuclear markers link a new green toad from Sicily to African relatives. BMC Evol Biol 8, 56.

Swenson, N.G., Howard, D.J., 2005. Clustering of contact zones, hybrid zones, and phylogeographic breaks in North America. Am. Nat. 166, 581–591.

Swofford, D.L., 2001. PAUP*4.0b: Phylogenetic Analysis Using Parsimony. Sinauer Associates, Sunderland.

Tajima, F., 1989. Statistical method for testing the neutral mutation hypothesis by DNA polymorphism. Genetics 123, 585–595.

Tamura, K., Peterson, D., Peterson, N., Stecher, G., Nei, M., Kumar, S., 2011. MEGA5: molecular evolutionary genetics analysis using maximum likelihood, evolutionary distance and maximum parsimony methods. Mol. Biol. Evol. 28, 2731–2739.

Tuniyev, B., 1999. A systematic list of amphibians from the Alpides of the Caucasus and Middle Asia, with comments on their taxonomy. Adv. Amphibian Res. Former Soviet Union 3, 43–75.

Veith, M., Steinfartz, S., Zardoya, R., Seitz, A., Meyer, A., 1998. A molecular phylogeny of "true" salamanders (family Salamandridae) and the evolution of terrestriality of reproductive modes. J. Zool. Syst. Evol. Res. 36, 7–16.

Veith, M., Fromhage, L., Kosuch, J., Vences, M., 2006. Historical biogeography of Western Palaearctic pelobatid and pelodytid frogs: a molecular phylogenetic perspective. Contr. Zool. 75, 109–120.

Vieites, D.R., Min, M., Wake, D.B., 2007. Rapid diversification and dispersal during periods of global warming by plethodontid salamanders. Proc. Natl. Acad. Sci. USA 104, 19903–19907.

Wielstra, B., Arntzen, J.W., 2011. Unraveling the rapid radiation of crested newts (*Triturus cristatus* superspecies) using complete mitogenomic sequences. BMC Evol. Biol. 11, 162.

Wielstra, B., Themudo, G.E., Güçlü, O., Olgun, K., Poyarkov, N.A., Arntzen, J.W., 2010. Cryptic crested newt diversity at the Eurasian transition: The mitochondrial DNA phylogeography of Near Eastern *Triturus* newts. Mol. Phylogenet. Evol. 56, 888–896.

Zeisset, I., Beebee, T.J.C., 2008. Amphibian phylogeography: a model for understanding historical aspects of species distributions. Heredity 101, 109–119.

Zhang, P., Papenfuss, T.J., Wake, M.H., Qu, L., Wake, D.B., 2008. Phylogeny and biogeography of the family Salamandridae (Amphibia: Caudata) inferred from complete mitochondrial genomes. Mol. Phylogenet. Evol. 49, 586–597.

Zwickl, D.J., 2006. Genetic Algorithm Approaches for the Phylogenetic Analysis of Large Biological Sequence Datasets under the Maximum Likelihood Criterion. Ph.D. dissertation. The University of Texas at Austin.